# Explosive cooperation in social dilemmas on higher-order networks

Andrea Civilini,[1,2] Onkar Sadekar,[3] Federico Battiston,[3] Jesús Gómez-Gardeñes,[4,5] and Vito Latora[1,2,6]

[1] *School of Mathematical Sciences, Queen Mary University of London, London E1 4NS, United Kingdom*
[2] *Dipartimento di Fisica ed Astronomia, Università di Catania and INFN, Catania I-95123, Italy*
[3] *Department of Network and Data Science, Central European University Vienna, Vienna 1100, Austria*
[4] *Department of Condensed Matter Physics, University of Zaragoza, 50009 Zaragoza, Spain*
[5] *GOTHAM lab, Institute of Biocomputation and Physics of Complex Systems (BIFI), University of Zaragoza, 50018 Zaragoza, Spain*
[6] *Complexity Science Hub Vienna, A-1080 Vienna, Austria*

Understanding how cooperative behaviours can emerge from competitive interactions is an open problem in biology and social sciences. While interactions are usually modelled as pairwise networks, the units of many real-world systems can also interact in groups of three or more. Here, we introduce a general framework to extend pairwise games to higher-order networks. By studying social dilemmas on hypergraphs with a tunable structure, we find an explosive transition to cooperation triggered by a critical number of higher-order games. The associated bistable regime implies that an initial critical mass of cooperators is also required for the emergence of prosocial behaviour. Our results show that higher-order interactions provide a novel explanation for the survival of cooperation.

*Introduction.* The pervasiveness of cooperation in our world has long puzzled researchers [1, 2]. After all, the natural world, and human society is not an exception, obeys Darwinian selection, which is driven by the self-interest of individuals. In such a competitive world, costly altruistic behaviours seem inappropriate, since they do not bring any immediate advantage to the cooperators [3–6]. It is instead more profitable for self-interested individuals to defect, exploiting the benefits from the actions of cooperators who, in turn, see their sustainability jeopardized by the higher profits of free-riders [7, 8].

Social dilemmas are a well-known theoretical framework for studying cooperation. In a social dilemma, each actor in a group can choose either to cooperate or to defect [9, 10]. Cooperating benefits the group at an individual cost, while defectors exploit collective benefits provided by cooperators without paying any cost [11, 12]. Therefore, while cooperation would be the best outcome from a group perspective, defection is the favoured strategy by selfish rational decision-makers. This tension between the two strategies defines the dilemma [13–16]. Social dilemmas are typically studied in evolutionary game theory [3, 7, 17–21] by implementing games, such as the Prisoner's Dilemma (PD), on structured populations [22–24]. The underlying structure of a population is usually modelled as a network, where links represent the interactions between pairs of agents [25–27]. In some cases, the structure of the network has been shown to promote prosocial behaviours through, e.g., mechanisms of network reciprocity [4, 28, 29], the heterogeneity of the nodes [30–33] and the presence of clustering [34]. Networks are however limited in their representation of real-world systems. The links of a network can indeed only describe pairwise interactions, while the units of a complex system can also interact in groups of more than two. Thus, networks do not allow to accommodate more realistic and general forms of higher-order social interactions.

In recent years, mathematical structures like hypergraphs and simplicial complexes have been used to represent interactions among three or more units [35–37]. From contagion processes [38] to synchronization [39–41] and ecological competition [42], various studies have illustrated that higher-order interactions can lead to the emergence of collective behaviours and dynamic patterns not seen in pairwise networks [36]. Since its origin [43], game theory has been formulated as an $n$-body problem. Therefore it comes as no surprise that higher-order interactions have attracted attention also in the study of evolutionary game theory [11, 44–50]. However, a general framework for social dilemmas on structured populations with group interactions is still missing. In fact, when higher-order payoffs for $n$-body games have been considered, it has been for well-mixed populations or for simple pairwise networks, such as regular lattices [12, 44, 45, 47, 51, 52]. When, instead, more general interaction patterns have been considered, it has been for specific problems and payoff structures relying on strong assumptions [50, 53, 54]. For example, when hypergraphs were used to model group interactions at the microscopic level [49, 55, 56], they often employed a linear function of the number of cooperators in a group as the group payoff, limiting the general representation of social dilemma dynamics [11].

In this Letter, we introduce a general framework to extend social dilemmas to structured populations accounting for interactions in groups of variable size. In our model, the players are the nodes of a hypergraph and are involved, at the same time, in both pairwise and higher-order games as represented by hyperedges of different sizes. We do so by assigning a payoff tensor of dimension $n$ to each hyperedge of size $n$. In this way, our model combines $n$-body games [12, 44, 45, 47, 57] with the potential of higher-order networks in representing the most general microscopic structure of the interactions [48, 55, 58, 59]. By studying the evolutionary dynamics of the model on

different types of hypergraphs, we find that the presence of higher-order interactions and their microscopic structure play an important role in the survival of cooperation in social dilemmas. In fact, above a critical number of higher-order interactions, the dynamics can show an explosive transition to a bistable state [60–62], where besides full defection (the only stable equilibrium for the pairwise PD) a cooperative stable state emerges. We provide an analytical characterization of the observed phase transition and its dependence on the parameters of the game. In particular, we found that an initial critical mass of cooperators is also needed to sustain cooperation in the long term: below this critical mass, every player becomes a defector, even if the number of higher-order interactions is above the critical threshold.

**The model.** We consider a population of $N$ players taking part in a number $M$ of different games, which can either be pairwise or in groups of three or more players. Such interactions are described by a hypergraph $\mathcal{H}(\mathcal{V},\mathcal{E})$, where $\mathcal{V}$ is the set of $|\mathcal{V}|=N$ nodes representing players, and $\mathcal{E}$ is the set of $|\mathcal{E}|=M$ hyperedges [35, 36]. Each hyperedge $e_g$, with $g\in\{1,\cdots,M\}$, is a group (a subset of $\mathcal{V}$) of two or more players interacting in game $g$. The hypergraph can be represented by an $N\times M$ incidence matrix $B$, whose entry $b_{ig}$ is equal to 1 if player $i$ is playing game $g$, and is zero otherwise. The number of games in which a player $i$ takes part is given by the hyperdegree $k_i=\sum_{g=1}^{M}b_{ig}$, while the number of players in a game $g$ is the size of the hyperedge $q_g=|e_g|=\sum_{i=1}^{N}b_{ig}$. We focus here on the case of hypergraphs with hyperedges of size two (2-hyperedges, or simply edges) and three (3-hyperedges), respectively corresponding to classical pairwise games (2-games) and games played in groups of three players (3-games). Regarding payoffs, since there are $q_g$ players involved in a symmetric game $g$, if we indicate as $n_s$ the number of different strategies available, the total number of different payoffs is $n_s\binom{n_s+(q_g-1)-1}{(q_g-1)}$ (see Supplemental Material, SM). Here we consider only $n_s=2$ possible strategies, cooperation (C) and defection (D), as in the classical pairwise social dilemmas, resulting in 4 possible different payoffs for 2-games and 6 for 3-games. As usual, the payoffs for 2-games can be displayed as a $2\times 2$ matrix $\Pi$, whose element $\pi_{s_is_j}=\left[\pi_{s_i}(s_j),\pi_{s_j}(s_i)\right]$ is the pair of payoffs for player $i$ and $j$ respectively, when the first player plays strategy $s_i$ and the second $s_j$. Generalizing to interactions in groups of three players, payoffs for 3-games can then be represented as a $2\times2\times2$ tensor $\mathcal{T}$, whose element $\tau_{s_is_js_k}=\left[\tau_{s_i}(s_j,s_k),\tau_{s_j}(s_i,s_k),\tau_{s_k}(s_i,s_j)\right]$ is now a 3-tuple with the value of the payoff for each of the three players $i$, $j$ and $k$, playing strategies $s_i$, $s_j$, $s_k$. The complete payoff structure for both 2-games ($q_g=2$) and 3-games ($q_g=3$) is shown in Fig. 1, using different symbols for different payoff values. As commonly done in the study of social dilemmas, without loss of generality we choose the payoff for mutual cooperation equal

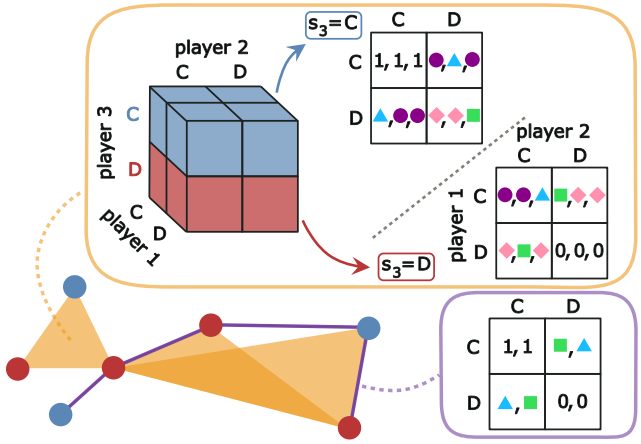


FIG. 1. Higher-order games on a hypergraph. The orange triangular areas are hyperedges of size $q_g=3$, corresponding to games played by three players (3-games), while the purple segments are hyperedges of size $q_g=2$, representing pairwise games (2-games). The payoff structures of symmetric 2-games and 3-games are reported in the two boxes.

1, while the payoff for mutual defection is equal 0, for both 2-games and 3-games [53]. In a similar manner, i.e. independently from the number of players (2 or 3) in the game, with ▲ and ■ we indicate the payoffs received for unilaterally deviating from mutual cooperation and defection respectively. In this way, it is immediate to identify in ▲ and in ■ the payoffs usually denoted, in pairwise social dilemmas, as the *temptation* $T$ and the *sucker*'s payoff $S$. Identifying $T$ and $S$ is crucial for the characterization of the game. The values of $T$ and $S$ classify classical pairwise games into four different types, each with different Nash Equilibria (NE): the Prisoner's Dilemma ($T>1$, $S<0$), the Chicken game ($T>1$, $S>0$), the Stag Hunt game ($S<0$, $T<1$) and the Harmony game ($S>0$, $T<1$) (see SM). Hence, we propose extending the same classification to 3-games. In 3-games there are two additional payoffs, for defection against a cooperator and a defector (◆ namely W), and for cooperation against a cooperator and a defector (● namely G). Depending on the relative value of these two additional payoffs (if $G>W$ or $G<W$) each type of 3-games is divided into two subsets with different Nash Equilibria. As shown in SM, by restricting $G$ and $W$ to the range $0\leq G,W\leq 1$ (as we do for our results) the resulting 3-games are social dilemmas [12, 63, 64].

**Stochastic simulations.** To investigate the effects of higher-order interactions on the equilibria of a system with $N$ players, we considered the following stochastic evolutionary game dynamics. We start with a population having an initial fraction $\rho_0$ of cooperators. At each time step, one player (the focal) is selected at random, and a second player (the model) is chosen among the neighbouring nodes on the hypergraph, connected to the focal player by hyperedges of any size. Each of the two selected

players plays a 2-game with all its neighbors connected through a 2-hyperedge, and a 3-game for each 3-hyperedge it takes part in. A 2-game is completely defined by the values of the payoff matrix entries $T$ and $S$, while the 3-game has the same $T$ and $S$ of the 2-game, but is also defined by the payoffs $G$ and $W$. In each game, the focal (respectively, the model) player earns a payoff based on its strategy and the strategies of the other players involved in that particular game. The total payoff $\pi_f$ of the focal player ($\pi_m$ of the model player) is the sum of all the game payoffs. The focal player has then the possibility to adopt the strategy of the model player $s_m$, with a probability which is a non-decreasing function of the total payoff difference $\pi_m - \pi_f$, modelled as a Fermi function [9, 19, 65]: $p_{s_f \to s_m} = \{1 + exp[-w(\pi_m - \pi_f)]\}^{-1}$ where $w$ represents the strength of selection [66]. We iterate the stochastic dynamics to compute the quasistationary (QS) probability distribution [67, 68] of the fraction of players adopting strategy $C$ (cooperators). This distribution is the stationary distribution of the stochastic process conditioned on non-extinction [69], and for a wide class of stochastic processes, its properties have been shown to converge to the stationary properties when $N \to \infty$ [70, 71]. In particular, in the context of evolutionary game theory, the QS distribution local maxima can converge, in unstructured populations and homogeneous random networks, to the stable fixed points $\rho^*$ of the mean-field deterministic evolution given by the replicator dynamics [50, 72]. As for the underlying structure of interactions, we have considered random hypergraphs in which we can control the number of higher-order interactions. By forming independently 2 and 3-hyperedges we have constructed random hypergraphs of $N$ nodes with tunable average hyperdegree $\langle k \rangle = \sum_{i=1}^{N} k_i/N$ and probability $\delta = n_\Delta/(N\langle k \rangle)$ for a player to interact in a 3-game. Here, $N\langle k \rangle = n_/ + n_\Delta$, where $n_/$ and $n_\Delta$ are respectively the number of 2-player interactions (the number of 2-hyperedges multiplied by 2) and the number of 3-player interactions (the number of 3-hyperedges multiplied by 3) in the system (see SM).

Fig. 2 shows the results for the case of the Prisoner's Dilemma (PD). We recall that the pairwise PD is defined by payoff values $T > 1$ and $S < 0$. In particular, for our simulations we chose $T = 1.1$, $S = -0.1$ and strength of selection $w = 1/\langle k \rangle$ [73]. As for the 3-game we consider a social dilemma with the same values of $T$ and $S$ of the pairwise PD, and with $G$ and $W$ such that $0 \leq G, W \leq 1$ and $(G - W) > 0$, since in this case the one-shot 3-game has 4 different pure NE: full defection (D,D,D) and all the permutations of 2 cooperators and 1 defector (see SM). Fig. 2(a) reports the fraction of cooperators at equilibrium as a function of the fraction $\delta$ of 3-game interactions, for different values of $a = 2(G - W)$. Symbols represent the simulation results obtained from the peaks of the QS distribution $p_{QS}(\rho)$ in panels (b-e). A bifurcation is observed when the fraction $\delta$ exceeds a critical value $\delta_c(a)$. For $\delta < \delta_c$ the only stable fixed point,

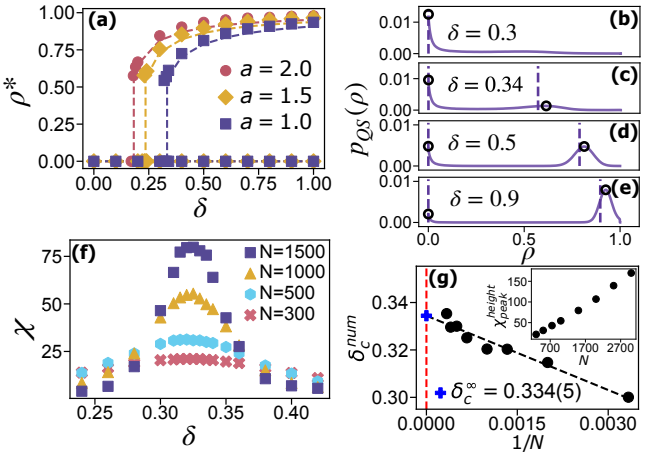


FIG. 2. **(a)** Fraction of cooperators at equilibrium for the PD on random hypergraphs with $N = 1500$, $\langle k \rangle = 20$ and tunable ratio $\delta$ of 3-player interactions. **(b-e)** Quasistationary distributions for $a = 1$ and four values of $\delta$. Continuous curves and symbols represent the simulation results averaged over 1500 runs, while dashed lines are the analytical mean-field predictions of Eqs. (3) and (4). **(f)** Susceptibility $\chi$ as a function of $\delta$ for increasing $N$. **(g)** Scaling of the position and height (inset) of the peak of $\chi$. The black line is the fitting.

as in the pairwise PD, is full defection $\rho^*_D = 0$ [74], while for $\delta \geq \delta_c$ we have bistability, with a new stable state $\rho^*_+$ appearing due to the effect of higher-order interactions. The observed phase transition is explosive [60–62] as, for $\delta \geq \delta_c$, the cooperative phase has $\rho^*_+ \geq 0.5$. To better characterize the phase transition we have computed the susceptibility $\chi = N\left(\langle \rho^2 \rangle - \langle \rho \rangle^2\right)$ as a function of $\delta$ for different hypergraph sizes $N$. In first-order transitions, this susceptibility peaks around the value of the control parameter where the new phase $\rho^*_+$ appears, and the peak diverges in the limit $N \to \infty$ because the system oscillates between the two phases [75]. Fig. 2(f) shows that, in our case, $\chi$ becomes more pronounced with increasing hypergraph size $N$. The critical value of $\delta$ in the thermodynamic limit can be extracted through a finite-size scaling analysis. The results are reported in Fig. 2(g), where $\delta_c^\infty = 0.334(5)$ is obtained as the y-intercept of the fitting of the critical $\delta_c^{num}(N)$ measured numerically (see SM) [75]. Fig. 3(a) illustrates the typical time evolution of the system. It reports the fraction of cooperators $\rho(t)$ as a function of time for 20 different initial conditions $\rho_0$. We notice that when $\rho_0$ is smaller than a given threshold $\rho^*_-$, the dynamics typically converges to the full defection state. Conversely, when $\rho_0 > \rho^*_-$, it converges to the stable state $\rho^*_+$ where a finite fraction of the population are cooperators. In other words, $\rho^*_-$ represents the initial critical mass of cooperators needed for cooperation to survive in the long term. Fig. 3(b) shows that $\rho^*_-$ is a decreasing function of $\delta$ for any value of the parameter $a$. This implies that smaller initial densities of cooperators are sufficient to sustain stable cooperation in systems

with a larger fraction $\delta$ of 3-game interactions (see SM for further details on the stochastic simulations). Notice that the results above depend on the topology of the hypergraph, as we found that a cooperative state is still possible, but the explosive transition for $\delta \geq \delta_c$ is replaced by a continuous one in the more constrained case of regular lattices with a tunable number of higher-order interactions (see SM).

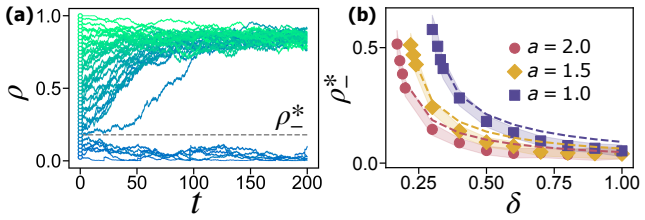


FIG. 3. Basins of attraction and critical mass of cooperators for the PD on random hypergraphs. **(a)** Temporal evolution of the fraction of cooperators for various initial conditions and $\delta = 0.4$, $a = 1.5$, $\langle k \rangle = 20$. **(b)** Unstable stationary state $\rho^*_-$ as a function of $\delta$ for average hyperdegree $\langle k \rangle = 20$ and different values of $a$. Symbols show the simulation results, while the lines are the analytical mean-field predictions. The shaded areas represent the errors.

**Analytical results.** To better understand the influence of higher-order interactions on the game outcome, we analytically examined the case of a well-mixed population, where each player interacts either in a 3-game with probability $\delta$ or in a 2-game with probability $1-\delta$. The dynamics of the fraction $\rho$ of cooperators for a well-mixed population in the thermodynamic limit is described by the mean-field Replicator Equation (RE) [7, 19, 76, 77]:

$$\frac{d\rho}{dt} = \rho(1-\rho)\left[\pi_C(\rho,\delta) - \pi_D(\rho,\delta)\right] \tag{1}$$

where $\pi_C$ and $\pi_D$ are the expected payoffs of a cooperator and a defector, functions of the density of cooperators $\rho$ and of the fraction $\delta$ of 3-game interactions (see SM). Hence, the payoff difference is also a function of $\rho$ and $\delta$:

$$\pi_C - \pi_D = -\rho^2 c\delta + \rho\,(c\delta - b - 2S) + S \tag{2}$$

where $c = (a+b)$, $b = T - S - 1$ and $a = 2(G-W)$. Therefore, besides the two absorbing states full-defection $\rho^*_D = 0$ and full-cooperation $\rho^*_C = 1$, Eq. 1 has two non-trivial stationary states $\rho^*_\pm$ for which $\pi_C - \pi_D = 0$:

$$\rho^*_\pm = \frac{c\delta - b - 2S \pm \sqrt{(c\delta - b)^2 + 4S(b+S)}}{2c\delta} \tag{3}$$

The existence of real-valued $\rho^*_\pm$ depends on the discriminant $\Delta = (c\delta - b)^2 + 4S(b+S) \geq 0$. Given that $(c\delta - b)^2$ is always positive, a sufficient condition for the existence is $4S(b+S) = 4S(T-1) > 0$, which is always satisfied for the Stag-Hunt game and Chicken game. For the Prisoner's Dilemma and the Harmony game instead $\Delta \geq 0$ holds only for certain values of the parameters. In particular, for the game we are focusing on in this Letter, namely the PD, we have $T > 1$ and $S < 0$, hence $b = T - S - 1 > 0$. Also, $c = a + b > 0$, as we are considering a 3-game with $a = 2(G-W) > 0$. This leads to positive real-valued $\rho^*_\pm$ when:

$$\delta \geq \delta_1^{\text{th}} = \frac{b + \sqrt{-4S(b+S)}}{c} \tag{4}$$

In particular, for $\delta = \delta_1^{\text{th}}$, where the two solutions $\rho^*_+$ and $\rho^*_-$ appear and coincide ($\Delta = 0$), they take the value $\rho^*_\pm(\delta_1^{\text{th}}) = 0.5 - (b+2S)/[2(b + \sqrt{-4S(b+S)})]$, while for $\delta > \delta_1^{\text{th}}$ we have $0 < \rho^*_- < \rho^*_\pm(\delta_1^{\text{th}}) < \rho^*_+ < 1$ (see SM). A stability analysis of the solutions reveals that, while $\rho^*_D = 0$ and $\rho^*_+$ are stable, $\rho^*_-$ and $\rho^*_C = 1$ are unstable stationary states. Therefore, Eq. (4) gives us the mean-field critical threshold $\delta_1^{\text{th}}$ of 3-player interactions for cooperation to survive in the higher-order PD. In fact, if $\delta$ is below this critical threshold the only stable stationary state is full defection $\rho^*_D = 0$, as in the pairwise PD. If instead the fraction of 3-game interactions $\delta$ exceeds $\delta_1^{\text{th}}$, an explosive transition to a bistable state emerges, where both $\rho^*_D = 0$ and $0 < \rho^*_+ < 1$ are stable stationary states. In Fig. 2(a-e) the analytical mean-field results are reported as dashed lines. In particular, the analytical predictions for the stable states $\rho^*_+$ and $\rho^*_D$ are in perfect agreement with the peaks of the quasistationary distributions in Fig. 2(b-e) and with the symbols in panel (a) reporting the stable fixed points obtained through stochastic simulations on random hypergraphs. At the same time, the critical fraction of 3-game interactions $\delta_1^{\text{th}}$ (vertical lines in Fig. 2(a)) accurately marks the discontinuous transition to bistability observed numerically, coinciding with the appearance of $\rho^*_\pm(\delta_1^{\text{th}})$. In particular, for the specific values of the parameters used in our simulations, we have $\delta_1^{\text{th}} = 0.\overline{3}$ and $\rho^*_\pm(\delta_1^{\text{th}}) = 0.5$, in perfect agreement with the simulation results. Fig. 3 displays the unstable solution $\rho^*_-$, which defines the basins of attraction of the two stable stationary states $\rho^*_D$ and $\rho^*_+$, showing again a good agreement between the mean-field predictions (dashed lines) and the stochastic simulations (trajectories in Fig. 3(a) and symbols in Fig. 3(b)).

*Conclusions.* In this Letter, we introduce a general game theory framework to study social dilemmas when both pairwise and higher-order interactions are possible. Our main finding is that cooperation can persist even in scenarios like the PD, where pairwise interactions typically lead to full defection. The transition to a stable cooperative state is explosive when the number of higher-order interactions surpasses a critical threshold determined by game parameters. The presence of bistability, however, indicates that the survival of cooperators is not guaranteed: a critical mass of initial cooperators is needed to sustain stable prosocial behaviour. This is in agreement with empirical observations regarding the critical mass of initiators required to trigger social and cultural changes

[78, 79]. Our findings show that higher-order interactions can foster cooperation in competitive settings, offering a novel solution to social dilemmas. While we focus on the PD in this Letter, our higher-order framework readily applies to other games. We also hope our work inspires systematic investigations into the impact of various real-world features, such as different topologies of higher-order networks and temporal changes in their connectivity, on evolutionary game dynamics.

*Acknowledgements.* The authors warmly thank Mark Broom for his helpful comments and suggestions. A.C. and V.L. acknowledge support from the European Union - NextGenerationEU, GRINS project (grant E63-C22-0021-20006). F.B. acknowledges support from the Air Force Office of Scientific Research under award number FA8655-22-1-7025. J.G.-G. acknowledges support from Departamento de Industria e Innovación del Gobierno de Aragón (FENOL group, grant E36-23R) and from Ministerio de Ciencia e Innovación de España through grant PID2020-113582GB-I00.

[1] R. Axelrod and W. D. Hamilton, Science **211**, 1390 (1981).
[2] M. A. Nowak and R. Highfield, *SuperCooperators: altruism, evolution, and why we need each other to succeed*, 1st ed. (Free Press, New York, NY, 2012).
[3] J. M. Smith and G. R. Price, Nature **246**, 15 (1973).
[4] M. A. Nowak and R. M. May, Nature **359**, 826 (1992).
[5] J. W. Weibull, *Evolutionary game theory*, 1st ed. (MIT Press, 2004).
[6] M. A. Nowak, *Evolutionary dynamics: exploring the equations of life* (Belknap Press of Harvard Univ. Press, 2006).
[7] J. Hofbauer and K. Sigmund, *Evolutionary Games and Population Dynamics*, 1st ed. (Cambridge University Press, 1998).
[8] M. Perc, J. J. Jordan, D. G. Rand, Z. Wang, S. Boccaletti, and A. Szolnoki, Phys. Rep. **687**, 1 (2017).
[9] G. Szabó and C. Tőke, Phys. Rev. E **58**, 69 (1998).
[10] M. Doebeli, C. Hauert, and T. Killingback, Science **306**, 859 (2004).
[11] M. Archetti and I. Scheuring, J. Theor. Biol. **299**, 9 (2012).
[12] M. Broom, K. Pattni, and J. Rychtář, Bull. Math. Biol. **81**, 4643–4674 (2019).
[13] G. Hardin, Science **162**, 1243 (1968).
[14] R. Axelrod and D. Dion, Science **242**, 1385 (1988).
[15] M. Milinski, D. Semmann, and H.-J. Krambeck, Nature **415**, 424 (2002).
[16] R. Dawkins, *The selfish gene*, 30th ed. (Oxford University Press, Oxford ; New York, 2006).
[17] J. M. Smith, *Evolution and the Theory of Games* (Cambridge University Press, 1982).
[18] H. Gintis, *Game Theory Evolving* (Princeton University Press, 2000).
[19] A. Traulsen, M. A. Nowak, and J. M. Pacheco, Phys. Rev. E **74**, 011909 (2006).
[20] A. Traulsen and C. Hauert, Stochastic evolutionary game dynamics, in *Reviews of Nonlinear Dynamics and Complexity*, Vol. 2 (John Wiley & Sons, Ltd, 2009) Chap. 2, pp. 25–61.
[21] M. Broom and J. Rychtář, *Game-Theoretical Models in Biology*, 2nd ed. (Chapman and Hall/CRC, 2022).
[22] G. Szabó and G. Fáth, Phys. Rep. **446**, 97 (2007).
[23] B. Allen, G. Lippner, Y.-T. Chen, B. Fotouhi, N. Momeni, S.-T. Yau, and M. A. Nowak, Nature **544**, 227 (2017).
[24] A. Antonioni and A. Cardillo, Phys. Rev. Lett. **118**, 238301 (2017).
[25] S. Boccaletti, V. Latora, Y. Moreno, M. Chavez, and D. Hwang, Phys. Rep. **424**, 175 (2006).
[26] M. Newman, *Networks* (Oxford University Press, 2010).
[27] V. Latora, V. Nicosia, and G. Russo, *Complex networks: principles, methods and applications*, 1st ed. (Cambridge University Press, 2017).
[28] E. Lieberman, C. Hauert, and M. A. Nowak, Nature **433**, 312 (2005).
[29] M. A. Nowak, Science **314**, 1560 (2006).
[30] F. C. Santos and J. M. Pacheco, Phys. Rev. Lett. **95**, 098104 (2005).
[31] F. C. Santos, J. M. Pacheco, and T. Lenaerts, Proc. Natl. Acad. Sci. U.S.A. **103**, 3490 (2006).
[32] J. Gómez-Gardeñes, M. Campillo, L. M. Floría, and Y. Moreno, Phys. Rev. Lett. **98**, 108103 (2007).
[33] F. C. Santos, M. D. Santos, and J. M. Pacheco, Nature **454**, 213 (2008).
[34] S. Assenza, J. Gómez-Gardeñes, and V. Latora, Phys. Rev. E **78**, 10.1103/PhysRevE.78.017101 (2008).
[35] F. Battiston, G. Cencetti, I. Iacopini, V. Latora, M. Lucas, A. Patania, J.-G. Young, and G. Petri, Phys. Rep. **874**, 1 (2020).
[36] F. Battiston, E. Amico, A. Barrat, G. Bianconi, G. Ferraz de Arruda, B. Franceschiello, I. Iacopini, S. Kéfi, V. Latora, Y. Moreno, M. M. Murray, T. P. Peixoto, F. Vaccarino, and G. Petri, Nat. Phys. **17**, 1093 (2021).
[37] F. E. Rosas, P. A. M. Mediano, A. I. Luppi, T. F. Varley, J. T. Lizier, S. Stramaglia, H. J. Jensen, and D. Marinazzo, Nat. Phys. **18**, 476 (2022).
[38] I. Iacopini, G. Petri, A. Barrat, and V. Latora, Nat. Commun. **10**, 2485 (2019).
[39] L. V. Gambuzza, F. Di Patti, L. Gallo, S. Lepri, M. Romance, R. Criado, M. Frasca, V. Latora, and S. Boccaletti, Nat. Commun. **12**, 1255 (2021).
[40] S. Stramaglia, T. Scagliarini, B. Daniels, and D. Marinazzo, Front. Physiol. **11**, 10.3389/fphys.2020.595736 (2021).
[41] L. Gallo, R. Muolo, L. V. Gambuzza, V. Latora, M. Frasca, and T. Carletti, Commun. Phys. **5**, 263 (2022).
[42] J. Grilli, G. Barabás, M. J. Michalska-Smith, and S. Allesina, Nature **548**, 210 (2017).
[43] J. Von Neumann and O. Morgenstern, *Theory of games and economic behavior* (Princeton University Press, 1944).
[44] M. Broom, C. Cannings, and G. Vickers, Bull. Math. Biol. **59**, 931 (1997).
[45] M. Bukowski and J. Miekisz, Int. J. Game Theory **33**, 41 (2004).
[46] C. E. Tarnita, T. Antal, H. Ohtsuki, and M. A. Nowak, Proc. Natl. Acad. Sci. U.S.A. **106**, 8601 (2009).
[47] C. S. Gokhale and A. Traulsen, Proc. Natl. Acad. Sci. U.S.A. **107**, 5500 (2010).
[48] M. Broom and J. Rychtář, J. Theor. Biol. **302**, 70 (2012).
[49] U. Alvarez-Rodriguez, F. Battiston, G. F. de Arruda, Y. Moreno, M. Perc, and V. Latora, Nat. Hum. Behav **5**, 586 (2021).

[50] A. Civilini, N. Anbarci, and V. Latora, Phys. Rev. Lett. **127**, 268301 (2021).
[51] J. Miekisz, Phys. A: Stat. Mech. Appl. **343**, 175 (2004).
[52] D. Kamiński, J. Miekisz, and M. Zaborowski, Bull. Math. Biol. **67**, 1195 (2005).
[53] H. Guo, D. Jia, I. Sendiña-Nadal, M. Zhang, Z. Wang, X. Li, K. Alfaro-Bittner, Y. Moreno, and S. Boccaletti, Chaos, Solit. Fractals **150**, 111103 (2021).
[54] Y. Xu, M. Feng, Y. Zhu, and C. Xia, Phys. A: Stat. Mech. Appl. **604**, 127698 (2022).
[55] J. Gómez-Gardeñes, M. Romance, R. Criado, D. Vilone, and A. Sánchez, Chaos **21**, 016113 (2011).
[56] A. Kumar, S. Chowdhary, V. Capraro, and M. Perc, Phys. Rev. E **104**, 054308 (2021).
[57] M. Dorraki, A. Allison, and D. Abbott, Sci. Rep. **9**, 8996 (2019).
[58] J. Gómez-Gardeñes, D. Vilone, and A. Sánchez, EPL **95**, 68003 (2011).
[59] M. Perc, J. Gómez-Gardeñes, A. Szolnoki, L. M. Floría, and Y. Moreno, J. R. Soc. Interface. **10**, 20120997 (2013).
[60] S. Boccaletti, J. Almendral, S. Guan, I. Leyva, Z. Liu, I. Sendiña-Nadal, Z. Wang, and Y. Zou, Phys. Rep. **660**, 1 (2016).
[61] R. M. D'Souza, J. Gómez-Gardeñes, J. Nagler, and A. Arenas, Adv. Phys. **68**, 123 (2019).
[62] C. Kuehn and C. Bick, Sci. Adv. **7**, eabe3824 (2021).
[63] M. Nowak, J. Theor. Biol. **299**, 1 (2012).
[64] J. Peña, B. Wu, and A. Traulsen, J. R. Soc. Interface **13**, 20150881 (2016).
[65] L. E. Blume, Games Econ. Behav. **5**, 387 (1993).
[66] We checked that birth-death and death-birth strategy update rules give results consistent with those obtained with the pairwise comparison process (see SM).
[67] M. M. de Oliveira and R. Dickman, Phys. Rev. E **71**, 016129 (2005).
[68] R. S. Sander, G. S. Costa, and S. C. Ferreira, Phys. Rev. E **94**, 042308 (2016).
[69] S. Méléard and D. Villemonais, Probab. Surv. **9**, 340 (2012).
[70] M. M. de Oliveira and R. Dickman, Phys. A: Stat. Mech. Appl. **343**, 525 (2004).
[71] M. Faure and S. J. Schreiber, J. Appl. Probab. **24**, 10.1214/13-AAP923 (2014).
[72] D. Zhou, B. Wu, and H. Ge, J. Theor. Biol. **264**, 874 (2010).
[73] We verified that the results are consistent for a range of $w$ spanning at least two orders of magnitude and for a wide range of average hyperdegree values (see SM).
[74] In the QS method, the system is prevented from visiting the absorbing states $\rho = 0$ and $\rho = 1$. As a consequence, the measured peak of the QS distribution cannot be in $\rho = 0$, but it is as close as it is allowed, in $\rho = 1/N$ which converges to 0 for large $N$.
[75] M. M. de Oliveira, M. G. E. da Luz, and C. E. Fiore, Phys. Rev. E **92**, 062126 (2015).
[76] A. Traulsen, J. C. Claussen, and C. Hauert, Phys. Rev. Lett. **95**, 238701 (2005).
[77] A. Traulsen, J. C. Claussen, and C. Hauert, Phys. Rev. E **74**, 011901 (2006).
[78] D. Centola, J. Becker, D. Brackbill, and A. Baronchelli, Science **360**, 1116 (2018).
[79] M. Pereda, V. Capraro, and A. Sánchez, Sci. Rep. **9**, 5503 (2019).
[80] For further details on the classification of higher-order social dilemmas, stochastic simulations, and analytical results, please refer to the SM available at [URL], which also includes Refs. [81–87].
[81] W. B. Liebrand, Simul. Gaming **14**, 123 (1983).
[82] B. Kerr, P. Godfrey-Smith, and M. Feldman, Trends Ecol. Evol. **19**, 135 (2004).
[83] F. Pedregosa, G. Varoquaux, A. Gramfort, V. Michel, B. Thirion, O. Grisel, M. Blondel, P. Prettenhofer, R. Weiss, V. Dubourg, J. Vanderplas, A. Passos, D. Cournapeau, M. Brucher, M. Perrot, and E. Duchesnay, J. Mach. Learn. Res. **12**, 2825 (2011).
[84] P. D. Taylor and L. B. Jonker, Math. Biosci. **40**, 145 (1978).
[85] P. Schuster and K. Sigmund, J. Theor. Biol. **100**, 533 (1983).
[86] L. Hindersin and A. Traulsen, PLoS Comput. Biol. **11**, e1004437 (2015).
[87] B. Wu, J. García, C. Hauert, and A. Traulsen, PLoS Comput. Biol. **9**, e1003381 (2013).

# Supplemental material for "Explosive cooperation in social-dilemmas on higher-order networks"

Andrea Civilini,[1,2] Onkar Sadekar,[3] Federico Battiston,[3] Jesús Gómez-Gardeñes,[4,5] and Vito Latora[1,2,6]

[1] *School of Mathematical Sciences, Queen Mary University of London, London E1 4NS, United Kingdom*
[2] *Dipartimento di Fisica ed Astronomia, Università di Catania and INFN, Catania I-95123, Italy*
[3] *Department of Network and Data Science, Central European University Vienna, Vienna 1100, Austria*
[4] *Department of Condensed Matter Physics, University of Zaragoza, Zaragoza, Spain*
[5] *GOTHAM lab, Institute of Biocomputation and Physics of Complex Systems (BIFI), University of Zaragoza, Zaragoza, Spain*
[6] *Complexity Science Hub Vienna, A-1080 Vienna, Austria*

## NUMBER OF DIFFERENT PAYOFFS

We consider a general $q_g$-person game, where each player can choose among $n_s$ different strategies. If the players are distinguishable (i.e. not identical) then there are $n_s^{q_g}$ possible different elements of the payoff tensor and for each element, there are $q_g$ possible different individual payoffs. That is, in the case of distinguishable players the maximum number of different payoffs $N_\pi^{max}$ is:

$$N_\pi^{max} = n_s^{q_g} q_g \tag{S.1}$$

Instead, if the players are identical, the payoff of a player depends on its strategy and on the unordered sample of the strategies of the other $q_g - 1$ players. Unordered because, since the players are identical, it does not matter which player plays which strategy. Given that there are $n_s$ possible different strategies, by applying the formula for unordered sampling with replacement of $q_g - 1$ items picked at random from $n_s$ choices, we find that for identical players (i.e. for symmetric games) the maximum number of different payoffs is:

$$N_\pi^{max} = n_s \binom{n_s + (q_g - 1) - 1}{(q_g - 1)} \tag{S.2}$$

Substituting, $q_g = 3$ and $n_s = 2$, we get $N_\pi^{max} = 6$. In our model we set the payoff for mutual cooperation $R = 1$ and that for mutual defection $P$ equals 0. The remaining four payoffs are then denoted as ●, ◆, ▲, and ■.

## CLASSIFICATION OF SOCIAL DILEMMAS

In a social dilemma each player can choose between two strategies, either to cooperate (strategy $C$) or to defect (strategy $D$) [1–3]. The dilemma arises from the inherent trade-off between these strategies. Opting to defect offers a higher individual payoff than cooperation when confronted by one or more cooperating players, allowing one to free-ride on the cooperative efforts of others. However, if all players collectively defect, it leads to a detrimental outcome for everyone, including the defectors, as the collective payoff diminishes. In the context of pairwise (2-player) social dilemmas, it is customary to set the payoffs for mutual cooperation (known as "Reward", denoted as $R$) and mutual defection (namely "Punishment", $P$) to 1 and 0, respectively. Moreover, the payoff associated with unilaterally deviating from mutual cooperation is $T$ ("Temptation"), while a player receives the payoff $S$ ("Sucker") for deviating from mutual defection. It follows that if $S > 0$ it is convenient for a rational player to deviate from mutual defection, while if $T > 1$ it is preferable to deviate from mutual cooperation. Therefore, depending on the combination of values of $T$ and $S$ (i.e, above or below the threshold values 1 and 0), we get four scenarios that depict four possible different games. These games are characterized by different Nash equilibria and can be conveniently represented as a "square of games" as shown in Fig. 1. In particular, a Prisoner's Dilemma arises for $T > 1, S < 0$, a Chicken game for $T > 1, S > 0$, a Stag Hunt game for $T < 1, S < 0$, and $T < 1, S > 0$ define a Harmony game.

A pairwise game can be represented using the so-called payoff matrix representation, where the element of the matrix $\pi_{s_i s_j} = \left[\pi_{s_i}(s_j), \pi_{s_j}(s_i)\right]$ is the pair of payoffs for player $i$ and $j$ respectively, when the first player plays strategy $s_i$ and the second $s_j$ [4]. For 3-player games, the payoff matrix is then substituted by a $2 \times 2 \times 2$ payoff tensor $\mathcal{T}$, whose element $\tau_{s_i s_j s_k} = \left[\tau_{s_i}(s_j, s_k), \tau_{s_j}(s_i, s_k), \tau_{s_k}(s_i, s_j)\right]$ is now a 3-tuple with the value of the payoff for each of the three players $i$, $j$ and $k$, playing strategies $s_i$, $s_j$, $s_k$. As shown in the first section of the SM, the number of possible different payoffs for 3-player symmetric games is equal to 6. The complete $2 \times 2 \times 2$ payoff tensor is visually represented in Figure 2. Consistently with the pairwise social dilemmas, we choose the payoff for full cooperation (i.e. strategy profile


FIG. 1. Games square showing the games defined by the combination of values of $T$ and $S$ above or below the thresholds given by the values of the payoffs $R$ and $P$. In particular, we choose $R = 1$ and $P = 0$, as commonly done in the study of social dilemma games. It is worth noticing that the constraints $2R - P$ and $2P - R$, respectively for $T$ and $S$, are not strictly required to have a social dilemma, but are usually added for the sake of symmetry in the representation.

$(C, C, C)$) equal to $(1, 1, 1)$ and the payoff for mutual defection (strategy profile $(D, D, D)$) equal to $(0, 0, 0)$. As shown in the manuscript, in a 3-player game the payoff ▲ for unilaterally deviating from mutual cooperation (respectively the payoff ■ for deviating from mutual defection) is analogous to the temptation payoff $T$ (respectively sucker's payoff $S$) in the pairwise social dilemma. In fact, as in pairwise games, in 3-person games it is advantageous for a rational player

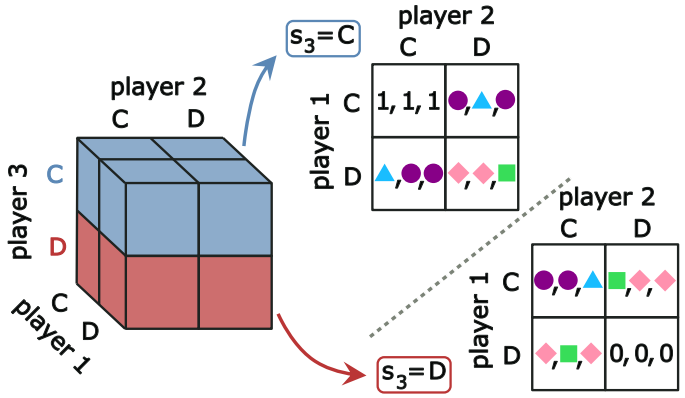


FIG. 2. Payoff tensor for 3-player social dilemmas. Consistently with the notation for pairwise games, we assume the payoffs for mutual cooperation and defection respectively equal to $(1, 1, 1)$ and $(0, 0, 0)$. The two matrices represent the two levels of the $2 \times 2 \times 2$ payoff tensor, whose elements are the triplets of payoffs $(\tau_1, \tau_2, \tau_3)$. The top matrix shows the payoffs when player 3 adopts cooperation, i.e. for $s_3 = C$. The matrix on the bottom reports the payoffs for the case $s_3 = D$. It is worth noticing that despite the game being symmetric it would be not obvious to reconstruct the whole payoff tensor just from the payoffs of player 1, as usually done in the case of pairwise symmetric games.

to deviate from mutual cooperation if ▲ $> R = 1$, while it is beneficial to deviate from mutual defection if ■ $> P = 0$. However, unlike the pairwise games, in 3-person games there are two additional payoffs (◆ and ●) that define a new threshold. In particular, if ◆ $>$ ●, it is favourable to be a defector when playing against a cooperator and a defector, while if ◆ $<$ ●, it is convenient to side with the cooperator.

### Classification of 3-player games

In light of their definitions, it becomes apparent that the payoffs ▲ and ■ represent the natural extension of $T$ and $S$ to the realm of 3-player games. To prevent any potential confusion, we propose to consistently refer to these 3-player counterparts using the same labels as their pairwise equivalents, specifically denoting ▲ as $T$ and ■ as $S$. With this alignment, we propose to extend the classification scheme based on the values of $T$ and $S$ from pairwise social dilemmas to 3-player games. Consequently, in 3-person games, we identify the same four social dilemmas that are recognizable in the pairwise case. However, the scenario becomes more complex for 3-player games, where the

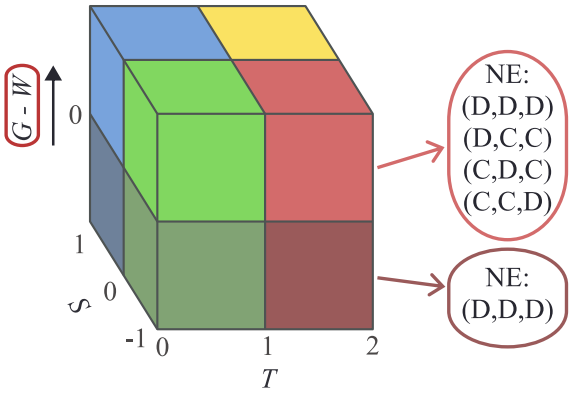


FIG. 3. Games cube showing the classification of 3-player symmetric games according to the values of the payoffs $T, S, G, W$. On the $T$ and $S$ axis we have the same restraints as for the pairwise games in Fig. 1, where we choose $R = 1$ and $P = 0$ as in the manuscript. However for 3-person games we have an extra dimension: depending on whether $G > W$ or $G < W$, each of the four pairwise games is now split in two distinct games with different NE. In the figure we show the different NE for the two HO PD, i.e. for the two disjoint subsets of 3-player games corresponding to the same values of $T$ and $S$ that define the pairwise PD ($T > 1$ and $S > 0$). The black arrow in the plot indicates the increasing direction of $G - W$.

relative magnitude of ● and ◆ now becomes an additional defining factor. This leads to a division of each of these four games into two separate subsets, each characterized by distinct Nash Equilibria. Consequently, the game square for pairwise games transforms into a game cube for 3-person games, as depicted in Fig. 3. The classification of 3-player games is detailed in the following list.

*3-player Prisoner's Dilemma game*

Pairwise Prisoner's Dilemma (PD) is defined by $T > 1$ and $S < 0$. For 3-player, the condition ● > ◆ defines two PD with different NE:

- ◆ > ●: $(D, D, D)$ is the only NE of the game.
- ◆ < ●: the game has 4 different pure NE, $(D, D, D)$, $(C, C, D)$, $(C, D, C)$, $(D, C, C)$.

*3-player Harmony game*

Pairwise Harmony games are defined by $T < 1$ and $S > 0$. Depending on the values of ● and ◆ we now have the following Nash Equilibria:

- ◆ > ●: the game has 4 different pure NE, $(C, C, C)$, $(C, D, D)$, $(D, C, D)$, $(D, D, C)$.
- ◆ < ●: $(C, C, C)$ is the only NE of the game.

*3-player Chicken game*

The pairwise Chicken game (CG) is defined by $T > 1$ and $S > 0$. The values of ◆ and ● characterize two different subsets of CG with different Nash Equilibria as:

- ◆ > ●: the NE are $(D, D, C)$, $(D, C, D)$ and $(C, D, D)$.
- ◆ < ●: the NE are $(C, C, D)$, $(C, D, C)$ and $(D, C, C)$.

*3-player Stag hunt game*

The Stag hunt game is defined by $T < 1$ and $S < 0$. In this case, the values of the payoffs ◆ and ● do not change the two NE, $(C, C, C)$ and $(D, D, D)$. However, depending on which payoff between ● and ◆ is higher, the ways in which is possible to reach these two NE changes, and one NE is favored over the other. In Game theory notation, this threshold influences the basin of attraction of the two NE, without changing the NE themselves, i.e. it makes one or the other NE risk dominant:

- ◆ > ●: there are more strategic moves leading to $(D, D, D)$ (it has a larger basin of attraction, i.e. it is risk dominant) than to $(C, C, C)$; defection is promoted over cooperation.
- ◆ < ●: cooperation is promoted since there are more strategic paths bringing to $(C, C, C)$.

## WHAT IS A SOCIAL DILEMMA?

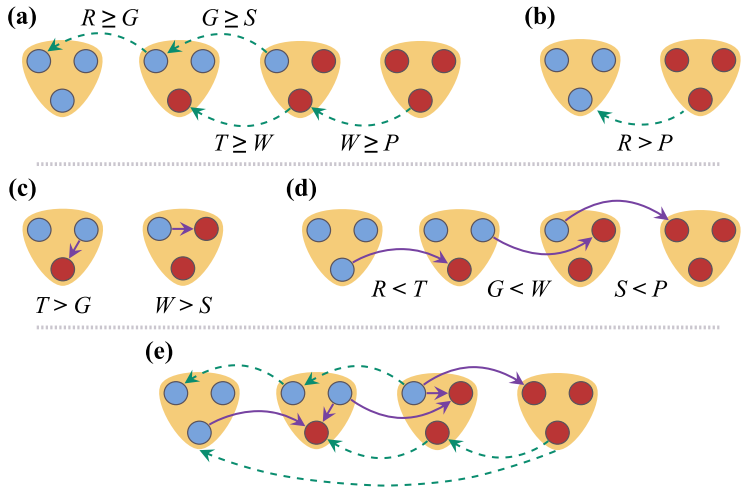


FIG. 4. Conditions for a 3-player social dilemma. **(a-b)**, payoffs restraints for having a *cooperation game*, as defined in Ref. [5]. The green dashed arrows are used to compare the payoffs of different players (dots), each arrow pointing in the direction of the higher payoff. These conditions on the payoff define what represents strategies of cooperation (in blue) and defection (red dots) in N-player games [6]. **(c, d)**, payoffs conditions defining the *temptation to defect*, as given in Ref. [7]. The purple solid arrows are used to compare the payoffs of different players (dots), each arrow pointing in the direction of the higher payoff. Differently from conditions **(a-b)**, in this case it is possible for the focal player (the node attached to the tail of the arrow) to change its strategy adopting the one of the player pointed by the arrow. **(e)**, by combining all the previous conditions we have a representation of a social dilemma, as defined in Ref. [6].

The game theory literature does not provide a universally agreed-upon definition of social dilemmas, with varying interpretations [5–9]. In our study, the concept of a higher-order social dilemma is grounded in the definition put forward by Ref. [6]. This definition hinges on a combination of two key conditions: first, a game must qualify as a *cooperation game*, which implies the identification of one strategy as cooperation and the other as defection [5]. Second, defection should be *tempting*, indicating that it is advantageous from a self-centered individual perspective but detrimental from a collective standpoint [7]. Fig. 4 illustrates this set of conditions for a 3-player game. More specifically, Fig. 4.**(a-b)** defines a cooperation game according to the criteria laid out in Ref. [5]:

**(a)** A focal player prefers other group members to cooperate, regardless of its own strategy:

$$\pi_C(j+1) \geq \pi_C(j) \text{ for } j = 0, 1, \ldots, d-2 \tag{S.3}$$
$$\pi_D(j+1) \geq \pi_D(j) \text{ for } j = 0, 1, \ldots, d-2 \tag{S.4}$$

where $\pi_X$ is the payoff of a focal player with strategy $X = C, D$, while $j$ represents the number of other group members (excluding the focal player) who are cooperators and $d$ is the size of the group. For $d = 3$ and using for

the payoffs the notation introduced in the manuscript, we have:

$$1 \geq G \geq S \tag{S.5}$$
$$T \geq W \geq 0 \tag{S.6}$$

**(b)** Mutual cooperation brings a higher payoff than mutual defection:

$$\pi_C(d-1) > \pi_D(0) \tag{S.7}$$

That for a 3-game reads:

$$1 > 0 \tag{S.8}$$

which is trivially satisfied for our choice of parameters, being 1 the payoff for mutual cooperation and 0 for mutual defection.

Panels **(c-d)** shows instead the conditions for the defection to be tempting, as presented in Ref. [7]:

**(c)** In a given group, defectors do better than cooperators:

$$\pi_D(j) > \pi_C(j-1) \text{ for } 0 < j < d-1 \tag{S.9}$$

By denoting the payoffs as in the manuscript, for a 3-game it gives:

$$T > G \tag{S.10}$$
$$W > S \tag{S.11}$$

**(d)** It is better to switch from cooperator to defector:

$$\pi_D(j) > \pi_C(j) \tag{S.12}$$

For a 3-game we have:

$$T > 1 \tag{S.13}$$
$$W > G \tag{S.14}$$
$$0 > S \tag{S.15}$$

According to Ref. [7], if all the conditions presented in **(c, d)** are satisfied, the game is deemed a *social dilemma*. Conversely, if only some of these conditions are met, the game falls into the category of a *relaxed social dilemma*. To exemplify, the pairwise Prisoner's Dilemma is classified as a social dilemma, while games like the pairwise Chicken game and the Stag Hunt game as relaxed social dilemmas, based on this categorization. Fig. 4.**(e)** combines together all the conditions, revealing the underlying tension inherent in social dilemmas. It visually depicts the conflict between a self-interested focal individual's actions aimed at maximizing its payoff, adopting the more profitable defection strategy (depicted by the purple solid arrows), and full cooperation, the more desirable outcome for the group, which remains elusive. In fact, the path towards full cooperation does not depend on the actions of the focal individual, but on the strategies adopted by the other members of the group (green dashed arrows). However, since also the other players are self-interested (as the focal individual) they will not cooperate just to increase the payoff of the focal, and the group will eventually reach the less desirable state of full defection.

### Is the higher-order (HO) PD a social dilemma?

We defined as HO PD the HO game with the same restriction on $T$ and $S$ of the pairwise PD, that is:

$$-1 < S < 0 \text{ and } 1 < T < 2 \tag{S.16}$$

For the pairwise PD these restraints are sufficient for having a social dilemma (i.e. the 2-game respects the conditions **(a-d)**). For the 3-player PD, we can obtain a social dilemma game, by adding restrictions to the payoffs $G$ and $W$ in order for the 3-game to respect conditions **(a-d)**. In particular, we can define a HO PD with $G - W > 0$ (the one that we used for the results in the manuscript), which satisfies all the conditions except obviously $W > G$ in **(d)**, simply by choosing $G$ and $W$ such that:

$$0 \leq W < G \leq 1 \tag{S.17}$$

or analogously:

$$0 < G - W \leq 1 - W, \text{ for } W \geq 0 \tag{S.18}$$

Therefore, with these restrictions, the HO PD with $G - W > 0$ is a *relaxed* social dilemma, according to Ref. [7]. It is worth noticing that the restraints given by Eq. (S.17) are sufficient, but not necessary, conditions for the payoffs to respect **(a,d)**. Moreover, they are sufficient for the 3-game to define a social dilemma only if Eqs. (S.16) also hold. Similarly, for the HO PD with $G - W < 0$, all the conditions **(a-d)** are satisfied if:

$$0 \leq G < W \leq 1 \tag{S.19}$$

or analogously:

$$G - 1 \leq G - W < 0, \text{ for } G \geq 0 \tag{S.20}$$

In this case, all the conditions **(a-d)** are satisfied, and then the 3-game PD with $G - W < 0$ is a social dilemma [7]. Fig. 5 shows the cube of 3-games with the new restrictions on $G, W$ given by Eqs.(S.17),(S.19), which make the HO PD a social dilemma. Similar conditions can be found to define HO (relaxed) social dilemma version of the Chicken, the Stag hunt and Harmony games.

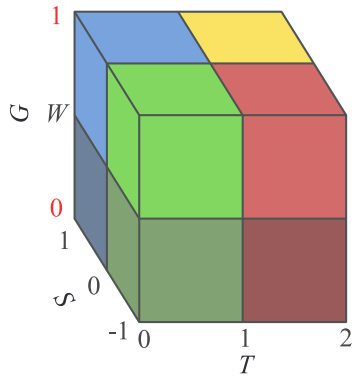


FIG. 5. Cube representing the classification of the 3-games depending on the values of the payoffs $T, S, G, W$, for $R = 1$ and $P = 0$. On the $G$ axis we added in red the restraints given by Eqs.(S.17),(S.19), and that are sufficient conditions for the HO PD (i.e, a 3-game with $T > 1$ and $S < 0$ as a pairwise PD) to be a social dilemma.

## GENERATING RANDOM HYPERGRAPHS

Before describing the procedure for generating random hypergraphs, let us introduce some standard hypergraph notation and provide an example of its application. As stated in the manuscript, we represent a population of $N$ players taking part in a number $M$ of different games as a hypergraph $\mathcal{H}(\mathcal{V}, \mathcal{E})$, where $\mathcal{V}$ is the set of $|\mathcal{V}| = N$ nodes

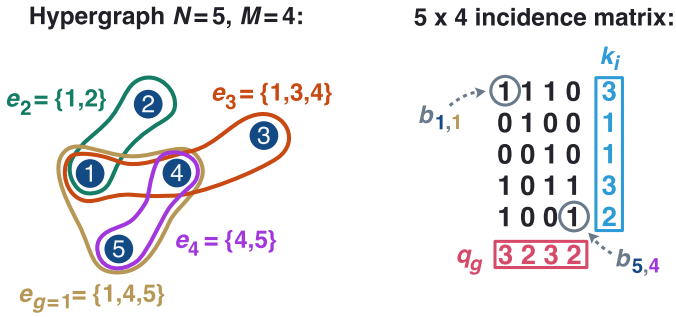


FIG. 6. A hypergraph with $N = 5$ nodes and $M = 4$ hyperedeges/groups (two 2-hyperedges and two 3-hyperedges) and its representation as a $5 \times 4$ incidence matrix. The nodes (blue circles) can belong to different hyperedeges (coloured lines) at the same time. If a node $i$ belongs to hyperedge $g$ the element of the incidence matrix $b_{i,g}$ is equal 1, otherwise is zero. The sum over the elements $b_{i,g}$ of the $i$-th row of the incidence matrix gives the hyperdegree of the $i$ node, while summing over the elements of the $g$-th column gives the size of the corresponding hyperedge. The total number of interactions can be computed as the sum over all the elements of the incidence matrix, and it is equal to $N\langle k\rangle = \sum_i \sum_g b_{i,g} = \sum_i (\sum_{g|q_g=2} b_{i,g} + \sum_{g|q_g=3} b_{i,g}) = n_/ + n_\Delta$. Therefore $n_/$ is the sum of the elements of the second and fourth columns, while $n_\Delta$ is the sum of the first and third columns corresponding to hyperedges of size 3. These definitions imply that $n_/$ and $n_\Delta$ correspond to the count of hyperedges of size 2 and 3, respectively, multiplied by their size (i.e. multiplied by 2 for 2-hyperedges and by 3 for 3-hyperedges). Hence, the total number of interactions in a system is equal to the number of hyperedges of a given size multiplied by the hyperedge size, and summed over all sizes.

representing players, and $\mathcal{E}$ is the set of $|\mathcal{E}| = M$ hyperedges [10, 11]. Each hyperedge $e_g$, with $g \in 1, \cdots, M$, represents a group (a subset of $\mathcal{V}$) of two or more players interacting in game $g$. The hypergraph can be represented by an $N \times M$ matrix, namely the incidence matrix $B$, whose entry $b_{i,g}$ is equal to 1 if player $i$ is playing game $g$, and is zero otherwise. Here, $i$ and $g$ are labels, with $i \in 1, \ldots, N$ identifying the node, while $g \in 1, \ldots, M$ identifying the game. The number of games in which a player $i$ takes part is given by its hyperdegree $k_i = \sum_{g=1}^{M} b_{i,g}$, while the number of players in a game $g$ is the size of the hyperedge $q_g = |e_g| = \sum_{i=1}^{N} b_{i,g}$. Fig. 6 illustrates a hypergraph of $N = 5$ nodes and $M = 4$ hyperedges, along with its representation as a $5 \times 4$ incidence matrix. In general, a player $i$ can take part in more games at the same time, and therefore for a given $i$, $b_{i,g}$ can be equal to 1 for different $g$. For instance, in the hypergraph represented in Fig. 6 player/node $i = 1$ belongs to hyperedges $e_{g=1}$, $e_2$ and $e_3$, and as a consequence $b_{1,1} = 1$, $b_{1,2} = 1$ and $b_{1,3} = 1$, while $b_{1,4} = 0$, since node 1 is not in hyperedge 4. By summing together the elements of the first row, we find the hyperdegree $k_1 = \sum_{g=1}^{4} b_{1,g} = 3$, while by performing the sum column-wise we find the size of the corresponding hyperedge. For example, by summing over the element of the first column we find the size $q_1$ of the hyperedge $e_1$, namely $q_1 = |e_1| = \sum_{i=1}^{5} b_{i,1} = 3$. We can also sum over the hyperdegree of all nodes $i$, finding the total hyperdegree, representing the total number of interactions in the system counted from a node/player perspective: $\sum_{i=1}^{N} k_i = \langle k\rangle N$, since the average hyperdegree $\langle k\rangle$ is, by its very definition, equal to $\langle k\rangle = \sum_{i=1}^{N} k_i/N$. In particular, in the study case considered in our manuscript, where only 2-player and 3-player games are allowed, one can count separately the contribution to the total number of interactions coming from 3-player games (i.e. hyperedges of size 3 or 3-games), denoted in the manuscript as $n_\Delta$, and instead from 2-games, denoted as $n_/$. That is, $N\langle k\rangle = n_\Delta + n_/$, where $n_\Delta \sum_i \sum_{g|q_g=3} b_{i,g}$ is the sum of the element of the incidence matrix restricted to hyperedeges of size 3, while $n_/ = \sum_i \sum_{g|q_g=2} b_{i,g}$ is restricted to groups of size 2. For example, considering the systems depicted in Fig. 6, we have: $N\langle k\rangle = \sum_i \sum_g b_{i,g} = \sum_i k_i = \sum_g q_g = 10$, $\langle k\rangle = \sum_{i=1}^{N} k_i/N = 2$, $n_\Delta = \sum_i \sum_{g|q_g=3} b_{i,g} = 6$, $n_/ = \sum_i \sum_{g|q_g=2} b_{i,g} = 4$.

We can now introduce the procedure employed to generate the random hypergraphs used as substrates for the simulations. As for the underlying structure of interactions, we have constructed random hypergraphs of size $N$ with tunable average hyperdegree $\langle k\rangle$ and numbers $n_/$, $n_\Delta$ of 2- and 3-player interactions, respectively. Let $\delta = n_\Delta/(n_\Delta + n_/)$, where $n_\Delta + n_/ = N\langle k\rangle$ is the total number of interactions in the hypergraph, be the probability for a player to interact in a 3-game. For fixed values of $N$, $\delta$ and $\langle k\rangle$, we start with $N$ nodes and first connect each of the possible $N(N-1)/2$ pairs of distinct nodes with a probability:

$$p_/ = (1-\delta)\langle k\rangle/(N-1) \tag{S.21}$$

We then connect each of the $N(N-1)(N-2)/6$ triplets of distinct nodes with a probability:

$$p_\Delta = 2\delta\langle k\rangle/((N-1)(N-2)) \tag{S.22}$$

Given that every time we add a pairwise edge the total hyperdegree of the network $N\langle k\rangle = \sum_{i=1}^{N} k_i$ (where $k_i$ is the hyperdegree of player $i$) increases by 2, while when we add a 3-hyperedge it increases by 3, we obtain a random hypergraph with the desired $\langle k\rangle$ and $\delta$. If the final hypergraph is not connected, we take the largest connected component. Fig. 7 shows that the networks obtained through this algorithm correctly reproduce the desired numbers of 2 and 3-player interactions, and average hyperdegree. In particular, in Fig. 7.a we notice that the numbers of 2-hyperedges and 3-hyperedges in which each player takes part in are distributed as binomial distributions centered around $k = 10$, as expected for random hypergraphs given the chosen parameters $\langle k\rangle = 20$ and $\delta = 0.5$ [12].

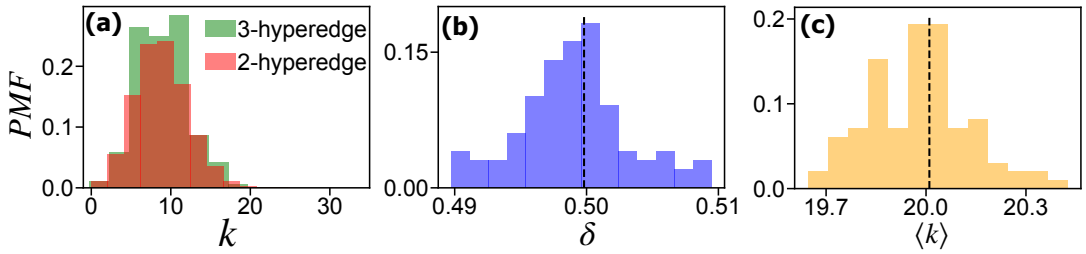


FIG. 7. **(a)** Probability mass function (PMF) of the hyperdegree $k$, distinguishing between the contribution to $k$ of 2-hyperedges and 3-hyperedges. **(b)** PMF of $\delta$, the fraction of 3-player interactions. **(c)** PMF of the average hyperdegree $\langle k\rangle$ of an hypergraph. The PMF are computed over 100 instances of a random hypergraph of size $N = 1500$. The dotted lines denote the mean of the distributions. The desired fraction of 3-hyperedges and average hyperdegree are $\delta = 0.5$ and $\langle k\rangle = 20$, respectively.

## DETAILS OF THE STOCHASTIC SIMULATIONS

### Stable states

In order to estimate $\rho_+^*$, we simulated 1500 runs of the stochastic evolutionary dynamics. For each run, we start with a randomly chosen fraction of cooperators $0 < \rho_0 < 1$ and we use a different instance of the random hypergraph. We use the quasistationary (QS) method [13, 14] to evolve the system allowing sufficient time for thermalization. In particular, for our simulations on hypergraphs of size $N = 1500$, we chose a thermalization time $t_{th} \approx N \times 10^3$ time steps and a total simulation length of $t_{tot} \approx N \times 10^4$ time steps. We recall from the manuscript that we are focusing on the case of the Prisoner's Dilemma and to define the game we chose the payoff values $T = 1.1$ and $S = -0.1$.

As for the strength of selection we chose $w = 1/\langle k\rangle$, however we have verified that the results are consistent for at least one order of magnitude above and below this choice for $w$. We chose $w$ proportional to $1/\langle k\rangle$ in order to have a comparable strength of selection among different hypergraphs with different $\langle k\rangle$, since the average payoff in the hypergraph increases with the average hyperdegree. The peaks of the QS probability distribution of players with a given strategy (in our case cooperation) converge for $N >> 1$ to the stable steady state of the deterministic dynamics [15, 16]. We therefore use the peak(s) of the QS probability distribution obtained by averaging the distribution of cooperators over all the 1500 runs to estimate $\rho_D^*$ and $\rho_+^*$, the stable stationary states of the deterministic dynamics. The peaks are pronounced local maxima of the QS distribution. According to the value of $\delta$ we observe either one local maximum at $\rho_{max1}$ (corresponding to the stable state $\rho_D^*$) or two local maxima at $\rho_{max1}$ and $\rho_{max2}$, respectively. In particular, as $\delta$ increases above a critical value $\delta_c$ a second peak appears in $\rho_{max2}$, corresponding to the stable state $\rho_+^*$. We considered the peak in $\rho_{max2}$ significant (i.e. $\rho_+^*$ appeared) if its size, relative to the size of the first peak in $\rho_{max1}$, is above a given threshold $\frac{P_{QS}(\rho_{max2})}{P_{QS}(\rho_{max1})} > r$. We chose $r = 0.02$ and we verified the consistency of our results over a range of $r \approx [0.01, 0.1]$.

To estimate the error on our measurements of the stable stationary states, we then applied the same procedure used to measure $\rho_D^*$ and $\rho_+^*$ to the QS probability distribution of each of the 1500 runs, obtaining in this way one value, $(\rho_D^*)_i$, or two values, $(\rho_D^*)_i$ and $(\rho_+^*)_i$, for each run $i$. Finally, we computed the absolute deviations of the values of $(\rho_D^*)_i$ and $(\rho_+^*)_i$ from the measured stable stationary states $\rho_D^*$ and $\rho_+^*$ respectively (i.e., from the corresponding peak of the QS distribution averaged over all 1500 runs). The median of these absolute deviations is taken as the error $\Delta$ on the estimate of the stable stationary state, that is:

$$\Delta\rho_D^* = \text{median}\left[|\rho_D^* - (\rho_D^*)_i|\right] \tag{S.23}$$

$$\Delta\rho_+^* = \text{median}\left[|\rho_+^* - (\rho_+^*)_i|\right] \tag{S.24}$$

### Unstable state (critical mass of cooperators)

Here, we describe how we numerically measured $\rho^*_-$, which represents the critical mass of cooperators required to sustain stable cooperation. As $\rho^*_-$ is the unstable solution of the replicator dynamics, we employed a different approach than the one used for finding the stable stationary states. The idea behind this method is that if the system starts with an initial fraction of cooperators $\rho_0 < \rho^*_-$ the trajectory in time of the evolutionary stochastic dynamics will typically converge to the absorbing state $\rho^*_D$, while the trajectories starting in $\rho_0 > \rho^*_-$ will converge to the non-trivial stable state $\rho^*_+$. Therefore, finding $\rho^*_-$ is equivalent to finding the basins of attraction of the two stable stationary states $\rho^*_D$ and $\rho^*_+$. In particular, by denoting as $B_D$ the sets of initial conditions $\rho_0$ converging to $\rho^*_D$ and as $B_+$ the basin of attraction for $\rho^*_+$, we expect:

$$\rho^*_- = |B_D|/(|B_D| + |B_+|) \tag{S.25}$$

where $|\cdot|$ represents the cardinality, i.e., the number of elements in the set.

To find the basins of attraction, we considered 2000 simulation runs divided into 50 batches consisting of 40 runs. As the initial fraction of cooperators for the 40 runs, we chose equally spaced values $\rho_0$ ranging from 0 to 1. For each batch $j$, we determine the peak(s) of the QS distribution for each of the 40 runs, following the method outlined in the section regarding the stochastic simulation results for the stable states. If there is only one peak at $\rho^*_D$, we stop the procedure. Instead, if $\rho^*_+$ exists, we proceed to find $\rho^*_-$. For each run $i$ in batch $j$, we compute $\langle\rho\rangle^j_i$, the average fraction of cooperators over the last $t_{stat} \approx \times N \times 10$ timesteps of the dynamics. Thus, for each batch $j$, we end up with 40 values of $\langle\rho\rangle^j_i$ distributed around $\rho^*_D$ and $\rho^*_+$ in two separate clusters $C^j_D$ and $C^j_+$, respectively. We then utilize the K-means clustering method [17] to computationally determine the two clusters. Each data point $\langle\rho\rangle^j_i$ is assigned to either $C^j_D$ or $C^j_+$, resulting in $|C^j_D| + |C^j_+| = 40$ for every batch $j$. Here, $|\cdot|$ represents the cardinality, i.e., the number of elements in the set. In other terms, $C^j_D$ and $C^j_+$ represent the basins of attraction of $\rho^*_D$ and $\rho^*_+$, respectively, given 40 equally spaced initial conditions $\rho_0$. Then, for each batch $j$, we estimate the unstable stationary state as:

$$\rho^*_-(j) = |C^j_D|/(|C^j_D| + |C^j_+|) \tag{S.26}$$

Finally, we computed the unstable stationary solution as the average over all the batches:

$$\rho^*_- = \frac{1}{50}\sum_{j=1}^{50} \rho^*_-(j) \tag{S.27}$$

and as the error on the estimate of $\rho^*_-$ we took the standard deviation:

$$\Delta\rho^*_- = \sqrt{\frac{1}{50-1}\sum_{j=1}^{50}\left[\rho^* - \rho^*_-(j)\right]^2} \tag{S.28}$$

## DETAILS OF THE ANALYTICAL RESULTS

We adopt an evolutionary game theoretic approach to describe a well-mixed population of players engaged in a higher-order game. At each time step a randomly selected player (namely the focal) interacts with probability $\delta$ with other two players in a 3-person game (namely 3-game) described by the payoff tensor in Fig. 2, while with probability $1-\delta$ it plays with another player in the pairwise version of the game (2-game). We recall that the 2-game is completely defined by the values of S and T since by definition the payoffs for mutual defection and mutual cooperation are 1 and 0 respectively. The focal player can adopt the strategy (i.e. cooperation $C$ or defection $D$) of another randomly selected player, namely the model player, with a probability that is a non-decreasing function of the payoff difference between the model and focal players. By denoting with $\rho(t)$ the fraction of cooperators in the population at time $t$ (i.e. $1-\rho(t)$ is the fraction of defectors), the evolution in time of the cooperators' fraction is given by the replicator equation [18, 19]:

$$\frac{d\rho}{dt} = \rho\left[\pi_C - \langle\pi\rangle\right] \tag{S.29}$$

where $\langle\pi\rangle = \rho\pi_C + (1-\rho)\pi_D$ is the average payoff, and $\pi_C$ and $\pi_D$ are the expected payoffs of a cooperator and a defector respectively. Substituting the expression for $\langle\pi\rangle$ in Eq. S.29 we get Eq. (1) in the manuscript, as follows:

$$\begin{aligned}\frac{d\rho}{dt} =&\rho\left[\pi_C - (\rho\pi_C + (1-\rho)\pi_D)\right]\\ =&\rho\left[(1-\rho)\pi_C - (1-\rho)\pi_D)\right]\\ =&\rho(1-\rho)\left[\pi_C - \pi_D\right]\end{aligned} \tag{S.30}$$

In particular, the expected payoffs for a cooperator $\pi_C$ and defector $\pi_D$ are given by:

$$\pi_C = (1-\delta)\left[\rho + (1-\rho)S\right] + \delta\left[\rho^2 + 2\rho(1-\rho)G + (1-\rho)^2 S\right] \tag{S.31}$$

$$\pi_D = (1-\delta)\left[\rho T\right] + \delta\left[\rho^2 T + 2\rho(1-\rho)W\right] \tag{S.32}$$

where G (●), W ( ◆ ), T ( ▲ ), and S ( ■ ) are the elements of the payoff tensor as shown in Fig. 2. Note that the expected payoffs are both functions of the density of cooperators $\rho$ and the fraction of 3-game interactions $\delta$. Besides the two trivial absorbing stationary states $\rho_D^* = 0$ and $\rho_C^* = 1$, Eq. S.30 has two other stationary states $\rho_\pm^*$ for which $\frac{d\rho}{dt} = 0$. We introduce the quantities $a := 2(G-W)$, $b := T - S - 1$ and $c := (a+b)$ to simplify the payoff difference as:

$$\pi_C - \pi_D = -\rho^2 c\delta + \rho(c\delta - b - 2S) + S \tag{S.33}$$

By solving $\pi_C - \pi_D = 0$ we find the non-trivial stationary solutions as

$$\rho_\pm^* = \frac{c\delta - b - 2S \pm \sqrt{(c\delta - b)^2 + 4S(b+S)}}{2c\delta} \tag{S.34}$$

It follows that when $\Delta = [c\delta - b]^2 + 4S(b+S) \geq 0$, then $\rho_\pm^*$ are real valued for every $b, c, \delta, S$. In particular, given that $[c\delta - b]^2$ is always positive, a sufficient condition for the existence of the stationary solutions is $4S(b+S) = 4S(T-1) > 0$, which is always satisfied for the Stag Hunt game and Chicken game. For the Prisoner's Dilemma and the Harmony game instead $\Delta \geq 0$ requires that the parameters satisfy certain conditions. If $c > 0$, these conditions are:

$$\delta \geq \delta_1^{\text{th}} := \frac{b + \sqrt{-4S(b+S)}}{c} \tag{S.35}$$

$$\delta \leq \delta_2^{\text{th}} := \frac{b - \sqrt{-4S(b+S)}}{c} \tag{S.36}$$

while if $c < 0$:

$$\delta \leq \delta_1^{\text{th}} := \frac{b + \sqrt{-4S(b+S)}}{c} \tag{S.37}$$

$$\delta \geq \delta_2^{\text{th}} := \frac{b - \sqrt{-4S(b+S)}}{c} \tag{S.38}$$

In particular, for the case under investigation in the manuscript, that is the Prisoner's Dilemma with $a > 0$ (and hence $c > 0$, see manuscript), it is easy to verify that if $d = c\delta - b - 2S < 0$, then $\rho_\pm^* < 0$. Instead if $d = c\delta - b - 2S > 0$, then $\rho_\pm^* > 0$. In particular, we have $d > 0$ when

$$\delta > \delta_+^{\text{th}} := \frac{b + 2S}{c} \tag{S.39}$$

It can be shown that $\delta_2^{\text{th}} < \delta_+^{\text{th}} < \delta_1^{\text{th}}$ and therefore we have positive real-valued stationary solutions $0 < \rho_\pm^* < 1$ only for $\delta \geq \delta_1^{\text{th}}$, since if $\delta \leq \delta_2^{\text{th}} < \delta_+^{\text{th}}$ the real-valued solutions are negative. We notice that in the interval $\delta_1^{\text{th}} \leq \delta \leq 1$, $\rho_+^*$ is a strictly increasing function of $\delta$, while $\rho_-^*$ is strictly decreasing. By substituting the expression for $\delta_1^{\text{th}}$ in Eq. (S.34) we find the value that the two (coinciding) non-trivial solutions assume when they emerge. This is:

$$\rho_\pm^*(\delta_1^{\text{th}}) = \frac{1}{2} - \frac{b + 2S}{2(b + \sqrt{-4S(b+S)})} \tag{S.40}$$

In particular, $\rho_\pm^*(\delta_1^{\text{th}}) > 0$ when

$$2S < \sqrt{-4S(b+S)} \tag{S.41}$$

which is always satisfied in the case of the Prisoner's Dilemma, given that for this game $S < 0$ and $b + S = T - 1 > 0$. Consequently, for the PD the appearance in $\delta_1^{\text{th}}$ of the non-trivial stationary solution $\rho_+^*$ is always abrupt.

## SCALING ANALYSIS

To characterize the phase transition, we have investigated the scaling with $N$ of the critical fraction of 3-games required for the emergence of the bistable state. Following the standard definition of susceptibility $\chi = N\left(\langle\rho^2\rangle - \langle\rho\rangle^2\right)$ we computed $\chi$ as a function of the control parameter $\delta$. To compute the susceptibility we performed extensive simulations of the stochastic dynamics, with a thermalization time $t_{th} = N \times 10^3$, total simulation time of $t_{tot} = N \times 10^4$ timesteps, and running for each value of $\delta$ 200 simulation runs for random initial conditions $\rho_0$, the initial fraction of cooperators, for $T = 1.1$, $S = -0.1$, $G = 0.8$, $W = 0.3$, and $\langle k\rangle = 20$. It is worth noticing that very long thermalization and simulation times are required in this case, because the susceptibility is extremely sensitive to fluctuations in the quasistationary distribution.

Results reported in Fig.8(a) show that the susceptibility peaks around the value $\delta \sim \delta_c$ where $\rho_+^*$ appears (e.g., for the parameters used for these results, the well-mixed prediction for $\delta_c$ is $\delta_{th}^1 = 0.\overline{3}$). Fig.8(b) shows the height of the peak of the susceptibility as a function of $N$. The fact that the peak of the susceptibility becomes more and more pronounced as $N$ increases is an indication of the existence of a phase transition. Moreover, this is an indication that at $\delta_c$ a new phase coexists with the full defection phase: the susceptibility diverges at $\delta_c$ because the system is oscillating between these two phases. This is the typical signature of a first-order phase transition [20]. The critical

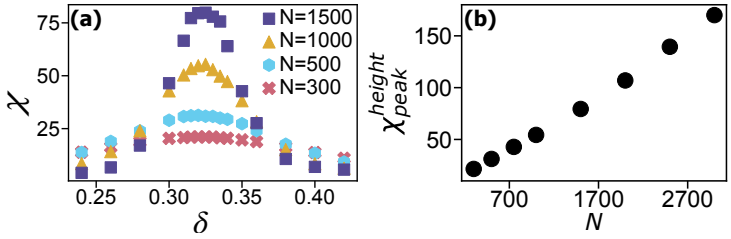


FIG. 8. (a) Susceptibility $\chi = N(\langle\rho^2\rangle - \langle\rho\rangle^2)$ as a function of $\delta$ for different sizes $N$ of the random hypergraph. (b) Scaling of the height of the susceptibility peak as a function of system size $N$. The parameters used for these simulations are $\langle k\rangle = 20$, $T = 1.1$, $S = -0.1$, $G = 0.8$, and $W = 0.5$.

value of $\delta$ in the thermodynamic limit can then be extracted through a finite-size scaling analysis. The results are reported in Fig. 9, where $\delta_c$ is estimated as the y-intercept $\delta_c^\infty$ of the fitting of the critical $\delta_c^{num}$ corresponding to different sizes $N$. In each panel, we used a different method to compute $\delta_c^{num}$, finding consistent results. In particular,

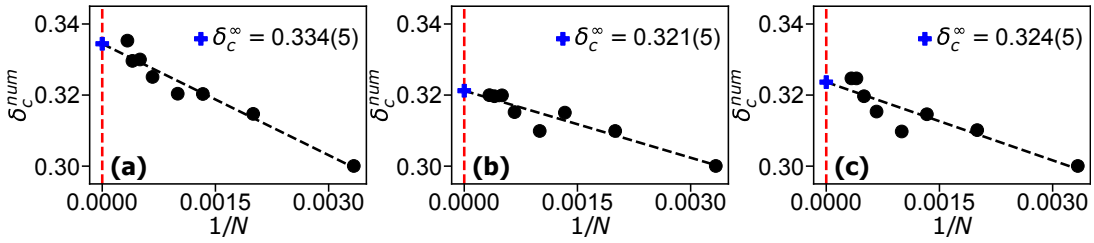


FIG. 9. Scaling of the numerically measured $\delta_c^{num}(N)$. The value of $\delta_c^\infty$ in the limit $N \to \infty$ is obtained as the y-intercept of the fitting. We found consistent results for three different methods used to compute $\delta_c^{num}$, namely: (a) peak of the susceptibility, (b) relative peaks' size, (c) equal area.

in panel (a) we show the value of $\delta_c^{num}$ corresponding to the peak of the susceptibility, while in panel (b) we measured $\delta_c^{num}$ as the minimum value of $\delta$ for which we have a ratio between the height of two peaks above a given threshold, that is when the second peak of the QS distribution $\rho_+^*$ is at least 1/50 times as high as the first peak (we also checked the consistency of this method for value of the threshold different from 1/50). Finally, in panel (c) we measured $\delta_c^{num}$ as the value of $\delta$ for which the areas around the two peaks of the bimodal QS distribution are equal [20].

## DIFFERENT STRATEGY UPDATE RULES

We tested the robustness of our findings under different update rules. We compared the *pairwise comparison process* used for the results in the manuscript with the *birth-death* and *death-birth* update dynamics. In fact, it has been

shown that different update rules can have a crucial impact on the outcome of the stochastic evolutionary dynamics on finite [21] and structured populations [22], depending on the game underlying the evolutionary dynamics and the network topology. We observe that for our framework the results are consistent among all the three update rules. In particular, the simulation results for both the pairwise comparison and the birth-death process on random hypergraphs are in excellent agreement with the analytic results for the replicator dynamics on well-mixed populations. For the death-birth process, we still observe a good qualitative agreement, with a slight enhancement in the level of cooperation observed for $\delta$ close to $\delta_c$ (i.e. where the bistable behaviour emerges), compared to the other two update rules.

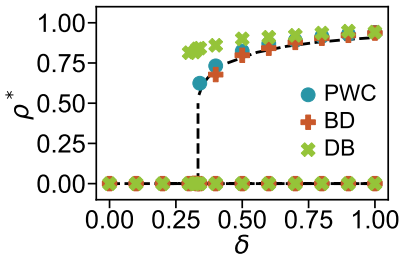


FIG. 10. Effect of different update rules on the numerical characterization of the dynamics' steady states on random hypergraphs. The pairwise comparison (PWC) and the birth-death (BD) processes show an excellent agreement and match very well the theoretical predictions of the deterministic replicator dynamics (dashed lines). The results for the death-birth (DB) process are still in good qualitative agreement, but the level of cooperation seems enhanced for $\delta$ close to $\delta_c$. The error bars are smaller than the size of the data points. In this case, the values of the parameters adopted are $G = 0.8$, $W = 0.3$, and $N = 500$.

## THE ROLE OF THE SELECTION STRENGTH AND OF THE AVERAGE HYPERDEGREE

We investigated how different levels of selection strength in strategy adoption impact the stable stationary states of the system. In the manuscript we compared the fraction of cooperators at equilibrium for the stochastic evolutionary dynamics on random hypergraph to the stable fixed points of the replicator equation, finding a very good agreement. We recall that in our model the probability of strategy adoption is given by the Fermi function $p_{s_f \to s_m} = \{1 + exp[-w(\pi_m - \pi_f)]\}^{-1}$ where $w$ represents the strength of selection, $s_f$ and $s_m$ are the strategies respectively of a focal and model player, $\pi_f$ and $\pi_m$ their payoffs. As shown in Ref. [23] for large unstructured populations, in general (i.e.

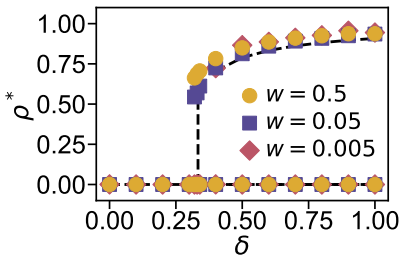


FIG. 11. Effect of different levels of selection strength $w$ on the numerical characterization of the stationary state(s). We observe that the results are very consistent for at least two orders of magnitude of the strength of selection and the stochastic simulation results (coloured dots) are in perfect agreement with the theoretical predictions (dashed lines) given by stable fixed points of the replicator equation. The error bars are smaller than the size of the data points. In this case, the values of the parameters adopted are $G = 0.8$, $W = 0.3$, $\langle k \rangle = 20$ and $N = 1500$.

for general strength of selection $w$) the strategies evolution under a strategy adoption probability given by the Fermi function can be approximated by a stochastic differential equation with a drift and a diffusion term:

$$\frac{d\rho}{dt} = \rho(1-\rho)\tanh\left(\frac{w}{2}(\pi_C - \pi_D)\right) + \sqrt{\frac{\rho(1-\rho)}{N}}\xi \tag{S.42}$$

where $\rho$ is the fraction of players with strategy $C$ (cooperation), $\pi_C$ and $\pi_D$ are the average payoff of a cooperator and defector respectively, $\xi$ is Gaussian white noise. This stochastic term vanishes in the limit $N \to \infty$, giving us:

$$\frac{d\rho}{dt} = \rho(1-\rho)\tanh\left(\frac{w}{2}(\pi_C - \pi_D)\right) \tag{S.43}$$

which in the limit $w << 1$ leads to the replicator equation:

$$\frac{d\rho}{dt} \propto \rho(1-\rho)\,(\pi_C - \pi_D) \tag{S.44}$$

We notice that Eq. (S.43) and Eq. (S.44) have the same stationary states: $\rho = 0, 1$ and $\rho$ such that $\pi_C - \pi_D = 0$, since $\tanh(x) = 0$ if and only if $x = 0$. This means that independently from the value of $w$ (i.e. also when the condition $w << 1$ does not hold) for sufficiently large $N$ on unstructured populations we expect to find identical stationary states. In Fig. 11 we report the stable stationary states found numerically, through stochastic simulations, for different orders of magnitude of the selection strength $w$ on random hypergraphs of size $N = 1500$. These results show that, even if in our simulations the population is structured, the strength of selection in this range of values does not impact significantly on the stable stationary states measured numerically, which remains in very good agreement with the theoretical predictions (i.e. the fixed points of the replicator equation) for all the values of $w$. It is worth stressing that these conclusions are not universal. In fact, it has been shown that, depending on the specific game and the strategy update rule, even in well-mixed populations the outcome of the evolutionary dynamics can vary with the strength of selection [24]. Thus, it remains crucial to assess how the system under investigation behaves at different selection intensity levels to determine the generality of the results and the robustness of the conclusions.

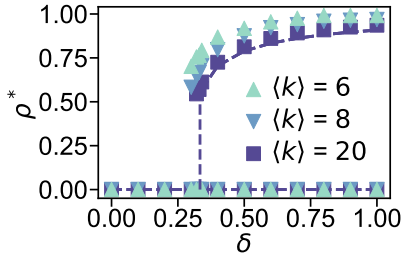


FIG. 12. Numerical characterization of the stationary state(s) for random hypergraphs with various average hyperdegrees $\langle k \rangle$. We observe consistent results for all the values of $\langle k \rangle$, in good agreement with the theoretical predictions (dashed lines) given by stable fixed points of the replicator equation. The error bars are smaller than the size of the data points. The values of the parameters adopted are G = 0.8, W = 0.3 and N = 1500.

For our simulations, both in this section and in the manuscript, we used random hypergraphs with an average hyperdegree $\langle k \rangle = 20$. To assess the impact of average hyperdegree on the model's outcome, we tested different values of $\langle k \rangle$. Fig. 12 displays the numerically measured steady states of the evolutionary dynamics for random hypergraphs with various values of $\langle k \rangle$, showing no significant differences in the results.

## REGULAR LATTICES

As we saw in the manuscript, the outcome of the evolutionary dynamics on random hypergraphs is in very good agreement with the predictions of the replicator equation (i.e. for a well-mixed infinite population). However, in this section we show that for different hypergraph topologies this is not always the case. In fact, as Fig.14 shows, taking as a substrate for the evolutionary dynamics a regular lattice with a tunable number of higher-order interactions completely changes the outcome of the model. To account for 3-body interactions, we considered two types of lattice: regular triangular lattices where each player is connected to exactly six neighbours, and double triangular (or Moore's) lattices, where each node is connected to eight neighbours (defining a so-called Moore's neighbourhood). To create a hypergraph, we start with a standard lattice, which has only pairwise interactions. We then define hyperedges of size 3, corresponding to 3-player games, by randomly selecting a fraction $p$ of the lattice's triangles and promoting them to higher-order interactions. To find the probability $p$ which gives us the desired fraction of higher-order interactions $\delta$, we start from the definition of $\delta$, given by $\delta = n_\Delta/(n_\Delta + n_/)$, where $n_\Delta$ represents the number of 3-player interactions, and $n_/$ denotes the interactions in 2-player games. An alternative definition is that $n_\Delta$ accounts for the contribution

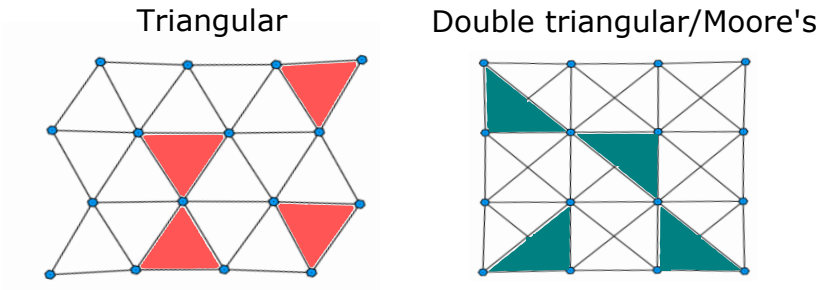


FIG. 13. The two regular lattices we have considered. A triangular lattice (left panel) where each node is connected to six neighbours and a double triangular lattice (right panel) where each node is connected to eight neighbours (defining a so-called Moore's neighbourhood). The links represent pairwise interactions and the colored triangles are 3-body interactions.

to the total hyperdegree from interactions in 3-player games, while $n_/$ represents the contribution from interactions in 2-player games. Each 2-hyperedge/game gives a contribution of 2 to the total hyperdegree, contributing 1 to the hyperdegree of each of the two players involved in the game. Given that the total number of 2-hyperedges is $e$, we have $n_/ = 2e$. Conversely, each 3-hyperedge contributes 3 to the total hyperdegree, as each 3-player game involves 3 players simultaneously. The total number of 3-hyperedges is $tp$, where $t$ denotes the total number of triangles in the lattice, and $p$ represents the fraction of these triangles that are promoted to 3-hyperedges. Hence, $n_\Delta = 3tp$. Substituting these values into the definition of $\delta$, we find:

$$\delta = \frac{3tp}{2e + 3tp} \tag{S.45}$$

Hence, we can express the parameter $p$ as a function of the desired $\delta$ as follows:

$$p = \frac{2\delta e}{(1-\delta)3t} \tag{S.46}$$

where $e$ is the number of distinguishable edges in the lattice, while $t$ represents the number of unique triangles in the lattice. It is straightforward to verify that the maximum possible value of $\delta$, denoted as $\delta_{max}$ and corresponding to $p = 1$ in Eq. (S.45), is given by:

$$\delta_{max} = \frac{3t}{2e + 3t} \tag{S.47}$$

For a triangular lattice of size $N$, where the number of different edges is $e \sim 3N$ and the number of distinguishable triangles $t \sim 2N$, we find that $\delta_{max} \approx 0.5$. This can be easily understood as follows. Each node $i$ is connected by a pairwise edge to 6 neighbours. This applies to all $N$ nodes, yielding a total of $6N$ pairs of neighbours [25]. However, if the order of the indices does not matter, among these $6N$ pairs of neighbours half are repeated, since if $i$ is a neighbour of $j$ then $j$ is also a neighbour of $i$. Therefore, the number of pairwise edges of an undirected triangular lattice, which represents the number of unique pairs, is $e \sim 6N/2$. Similarly, each node $i$ participates in 6 triangles with its neighbours, resulting in a total of $6N$ triangles in the network. However, if the order of indices does not matter, among the $6N$ triangles each unique triangle is counted 3 times: once for $j$ and $k$ neighbours of $i$, then for $k$ and $i$ neighbours of $j$, and finally for $j$ and $i$ as neighbours of $k$. As a consequence, the number of unique triangles, i.e. the maximum number of 3-hyperedeges in an undirected triangular lattice, is given by $t \sim 6N/3$. For double triangular (or Moore's) lattice instead, being $e \sim 4N$ and $t \sim 4N$, we have $\delta_{max} \approx 0.6$. We then characterized numerically the stable stationary states of the dynamics on regular lattices, following the same procedure used for random hypergraphs. In Fig. 13 we compare the results of the stochastic simulations for regular lattices to those for random hypergraphs. In particular, we observe that the discontinuous transition from pure defection to a cooperative state as a function of $\delta$ in the case of random hypergraphs, becomes a second-order (i.e., continuous) transition for lattices. One possible explanation for this difference is that on a regular lattice, the network effects are stronger compared to a random graph. The presence of shortcuts in a random graph leads to a slow growth of the graph's diameter $\phi$ with the size $N$, such as $\phi \sim \log(N)$ (the so-called small-world effect, [12]). On the other hand, on a lattice, the diameter grows as $\phi \sim N^{1/2}$. As a consequence, a dynamical process takes longer on a lattice to spread than on a random hypergraph. This means that a random hypergraph is closer to a mean-field population (where every individual can interact with everyone else, as in a fully connected network) than a lattice. Therefore, the better agreement with the predictions of

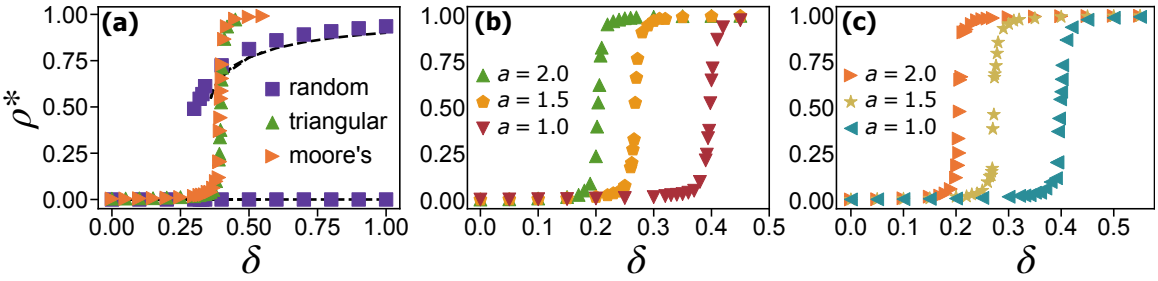


FIG. 14. Comparison of uniform random hypergraphs to triangular and double triangular (or Moore's) lattices. (a) The discontinuous transition to a bistable state observed on random hypergraphs and predicted by the mean-field replicator equation (dashed line) is replaced on regular lattices by a continuous transition to full cooperation. The results are consistent for various values of $G$ and $W$ for (b) triangular and (c) Moore's lattices.

the replicator equation is as expected. The high level of correlation between three players and two players interactions on the lattice could also play a significant role. In fact, in a lattice, for every 3-hyperedge there are necessarily three 2-hyperedges connecting the three nodes in the 3-hyperedge. This leads to correlation in the dynamics that are difficult to treat mathematically. In contrast, in a random hypergraph 3-hyperedges and 2-hyperedges are created through two independent processes. Consequently, in random hypergraphs, the number of 2-hyperedges, $k^i_{/}$, and of 3-hyperedge, $k^i_{\triangle}$, incident on each node $i$ are not correlated.

## BIFURCATION AS A FUNCTION OF $a$

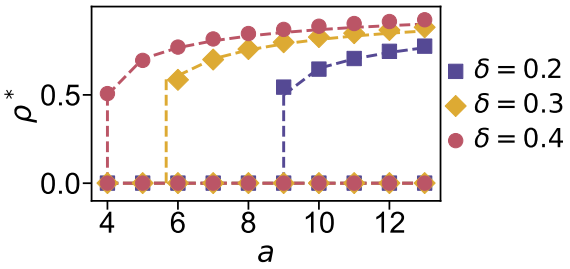


FIG. 15. Fraction of cooperators at equilibrium as a function of $a$ for average hyperdegree $\langle k\rangle = 20$ and different values of $\delta$. Symbols represent the stochastic simulation results averaged over 1500 independent runs (the error bars are smaller than the symbols), while dashed lines are the analytical mean-field predictions. For these results we choose $T = 1.5$ and $S = -0.5$.

In the section regarding the details of the analytical results, we found that the non-trivial stationary states $\rho^*_{\pm}$ described by Eq. S.34 exist (i.e., are real-valued and positive) iff $\delta > \delta_1^{\text{th}}$, where the critical threshold of 3-player interactions $\delta_1^{\text{th}}$ is a function of $a, b$ and $S$. However, the condition given by inequality Eq. (S.35) can also be expressed as a critical threshold on one of the other variables $a$, $b$, and $S$. For example, we can easily get a critical threshold on $a$ as a function of $\delta, b$ and $S$:

$$a > a_c = \frac{b(1-\delta) + \sqrt{-4S(b+S)}}{\delta} \tag{S.48}$$

Fig. 15 shows the bifurcation curve as a function of $a$ for various values of $\delta$. We observe a bifurcation in the stable points of the dynamics when $a = 2(G - W)$ exceeds a critical value $a_c$. In particular, while for $a < a_c$ the only stable NE is full defection $\rho^*_D$, as in the standard pairwise PD, for $a > a_c$ we observe the emergence of a bistable behaviour where cooperation survives: besides the full defection $\rho^*_D$, a new stable state $0 < \rho^*_+ < 1$ appears due to the effect of the payoffs associated with higher-order interactions.

## SYSTEMS WITH NO PAIRWISE GAMES (3-GAMES ONLY)

In our model we are "mixing" a fraction $1-\delta$ of interactions in pairwise PD with a fraction $\delta$ of interactions in higher-order games with the same payoffs $T$ and $S$ of the pairwise PD and with (DDD) and (DCC), (CDC),(CCD) as pure NE, as described in the main text. The characterization of the replicator dynamics (RD) for only 3-player games can be obtained as a special case of our framework by setting $\delta = 1$ (meaning that all the interactions are 3-player, with no pairwise games). Replacing $\delta = 1$ in Eq. (3) in the manuscript and following the procedure detailed in the SM's analytical section, we find that the non-trivial fixed points $\rho^*_\pm$ exist if and only if $\Delta = a^2 + 4S(b+S) > 0$. Substituting the definitions of $a$ and $b$ it is straightforward to derive the condition for the existence of the internal stationary states $\rho^*_\pm$ for the case $\delta = 1$ (i.e. for only 3-player games):

$$G - W > \sqrt{(1-T)S} \tag{S.49}$$

This condition is always satisfied for values of $G$, $W$, $T$ and $S$ for which we observe a bifurcation (i.e. the discontinuous transition to the bistable state) as a function of $\delta$. In fact, to have a bistable stationary state we need $\Delta = (c\delta - b)^2 + 4S(b+S) > 0$ (the $\Delta$ of Eq. (3) in the manuscript). By the very definition of $\delta^1_{th}$, we know that the condition $\Delta > 0$ is satisfied (and we observe the bistable state) $\forall \delta > \delta^1_{th}$, where $0 \leq \delta \leq 1$ is the fraction of 3-player interactions. Therefore, as long as the payoff $G$, $W$, $T$ and $S$ are such that $\delta^1_{th} < 1$, $\Delta(\delta = 1)$ is guaranteed to be greater than 0 and the corresponding condition on the payoffs $G - W > \sqrt{(1-T)S}$ holds true. As a consequence, whenever there are values of $\delta^1_{th} < \delta \leq 1$ for which we observe the bistable state, the symmetric 3-game in the "mixture" has two interior NE, as shown in Ref. [26].


[1] G. Szabó and C. Tőke, Phys. Rev. E **58**, 69 (1998).
[2] G. Szabó and G. Fáth, Phys. Rep. **446**, 97 (2007).
[3] M. Doebeli, C. Hauert, and T. Killingback, Science **306**, 859 (2004).
[4] J. W. Weibull, *Evolutionary game theory*, 1st ed. (MIT Press, 2004).
[5] J. Peña, B. Wu, and A. Traulsen, J. R. Soc. Interface **13**, 20150881 (2016).
[6] M. Broom, K. Pattni, and J. Rychtář, Bull. Math. Biol. **81**, 4643–4674 (2019).
[7] M. Nowak, J. Theor. Biol. **299**, 1 (2012).
[8] W. B. Liebrand, Simul. Gaming **14**, 123 (1983).
[9] B. Kerr, P. Godfrey-Smith, and M. Feldman, Trends Ecol. Evol. **19**, 135 (2004).
[10] F. Battiston, G. Cencetti, I. Iacopini, V. Latora, M. Lucas, A. Patania, J.-G. Young, and G. Petri, Phys. Rep. **874**, 1 (2020).
[11] F. Battiston, E. Amico, A. Barrat, G. Bianconi, G. Ferraz de Arruda, B. Franceschiello, I. Iacopini, S. Kéfi, V. Latora, Y. Moreno, M. M. Murray, T. P. Peixoto, F. Vaccarino, and G. Petri, Nat. Phys. **17**, 1093 (2021).
[12] M. Newman, *Networks* (Oxford University Press, 2010).
[13] M. M. de Oliveira and R. Dickman, Phys. Rev. E **71**, 016129 (2005).
[14] R. S. Sander, G. S. Costa, and S. C. Ferreira, Phys. Rev. E **94**, 042308 (2016).
[15] M. M. de Oliveira and R. Dickman, Phys. A: Stat. Mech. Appl. **343**, 525 (2004).
[16] D. Zhou, B. Wu, and H. Ge, J. Theor. Biol. **264**, 874 (2010).
[17] F. Pedregosa, G. Varoquaux, A. Gramfort, V. Michel, B. Thirion, O. Grisel, M. Blondel, P. Prettenhofer, R. Weiss, V. Dubourg, J. Vanderplas, A. Passos, D. Cournapeau, M. Brucher, M. Perrot, and E. Duchesnay, J. Mach. Learn. Res. **12**, 2825 (2011).
[18] P. D. Taylor and L. B. Jonker, Math. Biosci. **40**, 145 (1978).
[19] P. Schuster and K. Sigmund, J. Theor. Biol. **100**, 533 (1983).
[20] M. M. de Oliveira, M. G. E. da Luz, and C. E. Fiore, Phys. Rev. E **92**, 062126 (2015).
[21] A. Traulsen, J. C. Claussen, and C. Hauert, Phys. Rev. E **74**, 011901 (2006).
[22] L. Hindersin and A. Traulsen, PLoS Comput. Biol. **11**, e1004437 (2015).
[23] A. Traulsen, M. A. Nowak, and J. M. Pacheco, Phys. Rev. E **74**, 011909 (2006).
[24] B. Wu, J. García, C. Hauert, and A. Traulsen, PLoS Comput. Biol. **9**, e1003381 (2013).
[25] We are neglecting border effects, due to the finite size of the system, so these results are asymptotic approximations, true for $N \to \infty$.
[26] M. Bukowski and J. Miekisz, Int. J. Game Theory **33**, 41 (2004).